

One-loop quark and squark corrections to the lightest chargino pair production in photon-photon collisions *

Zhou Mian-Lai^b, Ma Wen-Gan^{a,b,c}, Han Liang^b, Jiang Yi^b and Zhou Hong^b

^aCCAST (World Laboratory), P.O.Box 8730, Beijing 100080, China.

^bDepartment of Modern Physics, University of Science and Technology of China (USTC), Hefei, Anhui 230027, China.

^cInstitute of Theoretical Physics, Academia Sinica, P.O.Box 2735, Beijing 100080, China.

*The project supported by National Natural Science Foundation of China

Abstract

We present the detailed analytical and numerical investigations of the one-loop radiative corrections of all quarks and their supersymmetric partners in the MSSM to the lightest chargino pair production via $\gamma\gamma$ fusion at the future NLC. The numerical results show that the cross sections of the subprocess and the parent process are typically enhanced by several percent compared to the results at the lowest order, and these corrections are mainly contributed by the virtual quarks and squarks of the third generation. Furthermore, we studied the effects induced by the CP violating complex phases stemming from squark and chargino mass matrices in the MSSM at one-loop level. We find that the radiative corrections are related to all the three CP violating complex phases $\phi_{t,b}$ and ϕ_μ . We conclude that the precise measurement of the cross section and the experimental determination of the parameters ϕ_μ and $\phi_{t,b}$ are crucial in searching for SUSY signals.

PACS number(s): 14.80.Ly, 12.15.Lk, 12.60.Jv

1. Introduction

The Standard Model(SM) [1] [2] can explain almost all the currently available experimental data pertaining to the strong, weak and electromagnetic interaction phenomena perfectly. The discovery of the top quark in 1995 by the CDF and D0[3] experiments at the Fermilab Tevatron once again confirmed the standard model(SM). Only the elementary Higgs boson, which is required strictly by the Standard Model for spontaneous symmetry breaking, remains to be found. Therefore, the SM is a successful theory of strong and electroweak interactions up to the present accessible energies. At present, the supersymmetric extended model(SUSY)[4] [20] is widely considered as theoretically the most appealing extension of the SM. Apart from describing the experimental data well, as the SM does, the supersymmetric theory is able to solve various theoretical problems, such as the fact that the SUSY may provide an elegant way to construct the huge hierarchy between the electroweak symmetry-breaking scale and the grand unification scales.

As we know, searching for sparticles directly at present and future colliders is one of the promising tasks[5], and the accurate measurements of the sparticle production process will give us significant information about the MSSM. Like other sparticles, charginos can also be produced in e^+e^- , $\gamma\gamma$ and hadron collisions. To detect the existence of charginos, e^+e^- and $\gamma\gamma$ collisions have an advantage over hadron collisions due to its cleaner background. So far there is no experimental evidence for charginos at LEP2. They only set lower bounds on the lightest chargino mass $m_{\tilde{\chi}_1^\pm}$. Recent experimental reports present that the mass of the lightest chargino may be larger than 85 GeV[8] [6][9], and this bound depends mainly

on the sneutrino mass and the mass difference between the chargino and the lightest SUSY particles(LSP) in theory.

The Next-generation Linear Collider(NLC) operated in laser back-scattering photon collision mode at a c.m.s. energy of $500 \sim 2000 \text{ GeV}$ with the luminosity of the order of $10^{33} \text{ cm}^{-2} \text{ s}^{-1}$ may be an ideal instrument to look for evidences of Higgs bosons and other new particles beyond the SM. The analysis for the production of chargino pair ($\tilde{W}^+ \tilde{W}^-$) via $\gamma\gamma$ collision at tree-level has been given in Ref.[24], and the production rate can be greater than that by direct e^+e^- annihilation, as the later has a ‘s-channel suppression’ due to the virtual photon propagator when the chargino is heavy. Therefore, $\gamma\gamma$ collision provides another way to produce chargino pair which is worth investigating.

We know that the precise measurements of chargino pair production rates and chargino masses give the possibility of measuring some gaugino, higgsino couplings and constraining the mass scale of squarks, which might not be in direct reach in colliders. Therefore, studying the chargino pair production in photon-photon fusion process only at the tree-level is far from the high precision requirements. Among all the radiative electroweak corrections within the MSSM for the process $\gamma\gamma \rightarrow \tilde{\chi}_1^+ \tilde{\chi}_1^-$, the one-loop contributions of the gaugino-higgsino-sector are very important. It is because not only the Yukawa couplings of these heavy quarks and squarks might enhance the correction, but also there exist the gaugino and higgsino couplings. In previous studies, the tree-level and complete one-loop calculations of heavy quarks and squarks for the chargino pair production in electron-positron collisions have been performed in references [10][11]. In Ref.[12] S. Kiyoura et.al. calculated the full quark and squark

one-loop corrections to $e^+e^- \rightarrow \tilde{\chi}_1^+ \tilde{\chi}_1^-$ and made comparisons with the results in [10]. There exist some numerical differences between their results[12], but they both concluded that the correction may be observable in chargino pair production at e^+e^- colliders.

In this work, we will investigate the full one-loop quark and squark corrections to the lightest chargino pair($\tilde{\chi}_1^+ \tilde{\chi}_1^-$) production via $\gamma\gamma$ fusion in the NLC within the MSSM. The paper is organized as follows: In section II we introduce the squark-sector and chargino-sector of the MSSM. In Sec.III we give the analytical results for the cross sections of subprocess $\gamma\gamma \rightarrow \tilde{\chi}_1^+ \tilde{\chi}_1^-$ at tree-level and the leading one-loop corrections involving virtual top, stop, bottom and sbottom quarks. In Sec.IV, the numerical results for subprocess and parent process are illustrated, along with discussions. Finally, a short summary is presented. In the Appendix, some lengthy expressions of the form factors which appear in the cross section in Sec.III are listed.

2. The squark-sector and chargino-sector of the MSSM and relevant Feynman rules.

In the MSSM theory every quark has two scalar partners, the squarks \tilde{q}_L and \tilde{q}_R . If there is no left-right flavor mixing in the squark-sector, the mass matrix of a scalar quark including CP-odd phases takes the following form[13]:

$$-\mathcal{L}_m = \begin{pmatrix} \tilde{q}_L^* & \tilde{q}_R^* \end{pmatrix} \begin{pmatrix} m_{\tilde{q}_L}^2 & a_q m_q \\ a_q^* m_q & m_{\tilde{q}_R}^2 \end{pmatrix} \begin{pmatrix} \tilde{q}_L \\ \tilde{q}_R \end{pmatrix}, \quad (2.1)$$

where \tilde{q}_L and \tilde{q}_R are the current eigenstates and for the up-type scalar quarks, we have

$$m_{\tilde{q}_L}^2 = \tilde{M}_Q^2 + m_q^2 + m_Z^2 \left(\frac{1}{2} - Q_q s_W^2 \right) \cos 2\beta, \quad (2.2)$$

$$m_{\tilde{q}_R}^2 = \tilde{M}_U^2 + m_q^2 + Q_q m_Z^2 s_W^2 \cos 2\beta, \quad (2.3)$$

$$a_q = |a_q| e^{-2i\phi_q} = \mu \cot \beta + A_q^* \tilde{M}. \quad (2.4)$$

For the down-type scalar quarks,

$$m_{\tilde{q}_L}^2 = \tilde{M}_Q^2 + m_q^2 - m_Z^2 \left(\frac{1}{2} + Q_q s_W^2 \right) \cos 2\beta, \quad (2.5)$$

$$m_{\tilde{q}_R}^2 = \tilde{M}_D^2 + m_q^2 + Q_q m_Z^2 s_W^2 \cos 2\beta, \quad (2.6)$$

$$a_q = |a_q| e^{-2i\phi_q} = \mu \tan \beta + A_q^* \tilde{M}, \quad (2.7)$$

where $Q_q (Q_D = -\frac{1}{3}, Q_U = \frac{2}{3})$ is the charge of the scalar quark, \tilde{M}_Q^2 , \tilde{M}_U^2 and \tilde{M}_D^2 are the self-supersymmetry-breaking mass terms for the left-handed and right-handed scalar quarks, $s_W = \sin \theta_W$, $c_W = \cos \theta_W$. We choose $\tilde{M}_Q = \tilde{M}_U = \tilde{M}_D = \tilde{M}$. $A_q \cdot \tilde{M}$ is a trilinear scalar interaction parameter, and μ is the supersymmetric mass mixing term of the Higgs boson. The complex value a_q can introduce CP-violation. In general, \tilde{q}_L and \tilde{q}_R are mixed and give the mass eigenstates \tilde{q}_1 and \tilde{q}_2 (usually we assume $m_{\tilde{q}_1} < m_{\tilde{q}_2}$). The mass eigenstates \tilde{q}_1 and \tilde{q}_2 are expressed in terms of the current eigenstates \tilde{q}_L , \tilde{q}_R and the mixing angle θ_q with the CP-violating phase ϕ_q . They read

$$\begin{aligned} \tilde{q}_1 &= \tilde{q}_L \cos \theta_q e^{i\phi_q} - \tilde{q}_R \sin \theta_q e^{-i\phi_q}, \\ \tilde{q}_2 &= \tilde{q}_L \sin \theta_q e^{i\phi_q} + \tilde{q}_R \cos \theta_q e^{-i\phi_q}, \end{aligned} \quad (2.8)$$

and

$$\tan 2\theta_q = \frac{2|a_q|m_q}{m_{\tilde{q}_L}^2 - m_{\tilde{q}_R}^2}. \quad (2.9)$$

Then the masses of \tilde{q}_1 and \tilde{q}_2 are

$$(m_{\tilde{q}_1}^2, m_{\tilde{q}_2}^2) = \frac{1}{2} \{ m_{\tilde{q}_L}^2 + m_{\tilde{q}_R}^2 \mp [(m_{\tilde{q}_L}^2 - m_{\tilde{q}_R}^2)^2 + 4|a_q|^2 m_q^2]^{\frac{1}{2}} \}. \quad (2.10)$$

The charginos $\tilde{\chi}_i^+$ ($i = 1, 2$) are four-component Dirac fermions which arise due to the mixing of the SUSY partners of the charged Higgs (charged Higgsinos \tilde{H}_1^- and \tilde{H}_2^+) and the W gauge bosons (the winos \tilde{W}^\pm). The chargino mass term in Lagrangian has the form

$$\mathcal{L}_m = -\frac{1}{2} (\psi^+ \ \psi^-) \begin{pmatrix} 0 & X^T \\ X & 0 \end{pmatrix} \begin{pmatrix} \psi^+ \\ \psi^- \end{pmatrix}. \quad (2.11)$$

where

$$X = \begin{pmatrix} M_{SU(2)} & m_W \sqrt{2} \sin \beta \\ m_W \sqrt{2} \cos \beta & |\mu| e^{i\phi_\mu} \end{pmatrix}, \quad (2.12)$$

and we set $M_{SU(2)}$ to be real because its complex phase angle can be rotated away by the field transformation and hence absorbed in ϕ_μ . The two 2×2 unitary matrices U, V are defined to diagonalize the matrix X , namely,

$$U^* X V^\dagger = X_D, \quad (2.13)$$

where X_D is a diagonal matrix with two non-negative entries M_\pm standing for the chargino masses $m_{\tilde{\chi}_{1,2}^+}$ at the tree level. The two diagonal elements of X_D are worked out in general case as

$$M_\pm^2 = \frac{1}{2} \left\{ M_{SU(2)}^2 + |\mu|^2 + 2m_W^2 \pm \left[(M_{SU(2)}^2 - |\mu|^2)^2 + 4m_W^4 \cos^2 2\beta + 4m_W^2 (M_{SU(2)}^2 + |\mu|^2 + 2M_{SU(2)} |\mu| \sin 2\beta \cos \phi_\mu) \right]^{1/2} \right\}, \quad (2.14)$$

Then the fundamental SUSY parameters $M_{SU(2)}$ and $|\mu|$ can be obtained from the alternative expressions on the right-hand side of the following equation, respectively.

$$(M_{SU(2)}, |\mu|) = \frac{1}{2} \left(\sqrt{m_{\tilde{\chi}_1^+}^2 + m_{\tilde{\chi}_2^+}^2 - 2m_W^2} + 2M_c \pm \sqrt{m_{\tilde{\chi}_1^+}^2 + m_{\tilde{\chi}_2^+}^2 - 2m_W^2 - 2M_c} \right), \quad (2.15.1)$$

where

$$M_c = m_W^2 \cos \phi_\mu \sin 2\beta + \sqrt{m_{\tilde{\chi}_1^+}^2 m_{\tilde{\chi}_2^+}^2 - m_W^4 \sin^2 2\beta \sin^2 \phi_\mu}. \quad (2.15.2)$$

The diagonalizing matrices U and V generally have the forms:

$$U = \begin{pmatrix} \cos \theta_U e^{i(\phi_1 + \xi_1)} & \sin \theta_U e^{i(\phi_1 + \xi_1 + \delta_U)} \\ -\sin \theta_U e^{i(\phi_2 + \xi_2 - \delta_U)} & \cos \theta_U e^{i(\phi_2 + \xi_2)} \end{pmatrix}$$

$$V = \begin{pmatrix} \cos \theta_V e^{i(\phi_1 - \xi_1)} & \sin \theta_V e^{i(\phi_1 - \xi_1 + \delta_V)} \\ -\sin \theta_V e^{i(\phi_2 - \xi_2 - \delta_V)} & \cos \theta_V e^{i(\phi_2 - \xi_2)} \end{pmatrix}, \quad (2.16)$$

where the ξ_1 and ξ_2 can be any arbitrarily chosen phases. It indicates that the matrices U and V satisfying Eq.(2.13) are not unique, namely, some arbitrary phases can be introduced but they have no physical effect. The explicit forms of the related constant angles and phases depending on the input parameters are given as

$$\tan \theta_U = \sqrt{\frac{M_+^2 - M_{SU(2)}^2 - 2m_W^2 \sin^2 \beta}{M_+^2 - |\mu|^2 - 2m_W^2 \cos^2 \beta}},$$

$$\tan \theta_V = \sqrt{\frac{M_+^2 - M_{SU(2)}^2 - 2m_W^2 \cos^2 \beta}{M_+^2 - |\mu|^2 - 2m_W^2 \sin^2 \beta}},$$

$$e^{i2\phi_1} = \frac{\cos \theta_U}{\cos \theta_V} \cdot \frac{M_+^2 + M_{SU(2)} |\mu| \tan \beta e^{i\phi_\mu} - 2m_W^2 \sin^2 \beta}{M_+ (M_{SU(2)} + |\mu| \tan \beta e^{i\phi_\mu})},$$

$$e^{i2\phi_2} = \frac{\cos \theta_V}{\cos \theta_U} \cdot \frac{M_-^2 + M_{SU(2)} |\mu| \tan \beta e^{i\phi_\mu} - 2m_W^2 \sin^2 \beta}{M_- (M_{SU(2)} \tan \beta + |\mu| e^{-i\phi_\mu})},$$

$$\begin{aligned}
e^{i\delta_U} &= \frac{M_{SU(2)} + |\mu|e^{i\phi_\mu} \tan \beta}{|M_{SU(2)} + |\mu|e^{i\phi_\mu} \tan \beta|}, \\
e^{i\delta_V} &= \frac{M_{SU(2)} \tan \beta + |\mu|e^{i\phi_\mu}}{|M_{SU(2)} \tan \beta + |\mu|e^{i\phi_\mu}|},
\end{aligned} \tag{2.17}$$

where M_\pm can be evaluated from Eq.(2.14). In the MSSM, there are many approaches to introduce CP-odd phases[14]. In our calculation, only two kinds of CP-odd phases, respectively appearing in the squark mass and chargino mass matrices, are involved. Although the detailed analyses of the present upper bounds on electron and neutron electric dipole moments may give constraints on CP-odd phase parameters indirectly[15], yet these constraints should be rather weak, since they depend strongly on the assumptions to be applied. Recently S.Y. Choi et al discussed the impacts of the CP-odd phase stemming from chargino mass matrix in the production of the lightest chargino-pair in e^+e^- collisions at tree-level[16]. In our work we are to investigate the effects from the CP-odd phases in squark mass and chargino mass matrices in the process of the lightest chargino pair production in $\gamma\gamma$ collisions at one-loop level. So we keep all the relevant CP-odd complex phases and do not put any extra limitations on CP-odd phases for the general discussion in our calculation.

The Feynman rules for the couplings of $q - \tilde{q}'_{L,R} - \tilde{\chi}_1^+$ are presented in Ref.[4][20]. Then we can obtain the corresponding Feynman rules for such vertices in squark mass eigenstate basis(see Fig.2). We denote the couplings in Fig.2 in the forms of

$$\bar{U} - \tilde{D}_i - \tilde{\chi}_j^+ : V_{U\tilde{D}_i\tilde{\chi}_j^+}^{(1)} P_L + V_{U\tilde{D}_i\tilde{\chi}_j^+}^{(2)} P_R, \tag{2.18.1}$$

$$U - \tilde{\bar{D}}_i - \tilde{\bar{\chi}}_j^+ : -V_{U\tilde{\bar{D}}_i\tilde{\bar{\chi}}_j^+}^{(2)*} P_L - V_{U\tilde{\bar{D}}_i\tilde{\bar{\chi}}_j^+}^{(1)*} P_R, \tag{2.18.2}$$

$$D - \bar{U}_i - \bar{\chi}_j^{+c} : C^{-1} \left\{ V_{D\bar{U}_i\bar{\chi}_j^+}^{(1)} P_L + V_{D\bar{U}_i\bar{\chi}_j^+}^{(2)} P_R \right\}, \quad (2.18.3)$$

$$\bar{D} - \tilde{U}_i - \tilde{\chi}_j^{+c} : \left\{ V_{D\tilde{U}_i\tilde{\chi}_j^+}^{(2)*} P_L + V_{D\tilde{U}_i\tilde{\chi}_j^+}^{(1)*} P_R \right\} C, \quad (2.18.4)$$

respectively. Here $(U, D) = (u, d), (c, s), (t, b)$ and C is the charge conjugation matrix, which appears when there is a discontinuous flow of fermion number, $P_{L,R} = \frac{1}{2}(1 \mp \gamma_5)$ and

$$V_{U\bar{D}_1\bar{\chi}_j^+}^{(1)} = \frac{igm_U}{\sqrt{2}m_W \sin \beta} V_{j2}^* \cos \theta_D e^{-i\phi_D}, \quad (2.19.1)$$

$$V_{U\bar{D}_1\bar{\chi}_j^+}^{(2)} = -ig(U_{j1} \cos \theta_D e^{-i\phi_D} + \frac{m_D}{\sqrt{2}m_W \cos \beta} U_{j2} \sin \theta_D e^{i\phi_D}), \quad (2.19.2)$$

$$V_{U\bar{D}_2\bar{\chi}_j^+}^{(1)} = \frac{igm_U}{\sqrt{2}m_W \sin \beta} V_{j2}^* \sin \theta_D e^{-i\phi_D}, \quad (2.19.3)$$

$$V_{U\bar{D}_2\bar{\chi}_j^+}^{(2)} = -ig(U_{j1} \sin \theta_D e^{-i\phi_D} - \frac{m_D}{\sqrt{2}m_W \cos \beta} U_{j2} \cos \theta_D e^{i\phi_D}), \quad (2.19.4)$$

$$V_{D\tilde{U}_1\tilde{\chi}_j^+}^{(1)} = ig(V_{j1}^* \cos \theta_U e^{i\phi_U} + \frac{m_U}{\sqrt{2}m_W \sin \beta} V_{j2}^* \sin \theta_U e^{-i\phi_D}), \quad (2.20.1)$$

$$V_{D\tilde{U}_1\tilde{\chi}_j^+}^{(2)} = \frac{-igm_D}{\sqrt{2}m_W \cos \beta} U_{j2} \cos \theta_U e^{i\phi_D}, \quad (2.20.2)$$

$$V_{D\tilde{U}_2\tilde{\chi}_j^+}^{(1)} = ig(V_{j1}^* \sin \theta_U e^{i\phi_U} - \frac{m_U}{\sqrt{2}m_W \sin \beta} V_{j2}^* \cos \theta_U e^{-i\phi_D}), \quad (2.20.3)$$

$$V_{D\tilde{U}_2\tilde{\chi}_j^+}^{(2)} = \frac{igm_D}{\sqrt{2}m_W \cos \beta} U_{i2} \sin \theta_U e^{-i\phi_D}, \quad (2.20.4)$$

For the Feynman rules of the Higgs-quark-quark, Higgs-squark-squark, Higgs-chargino-chargino and $Z(\gamma)$ -chargino-chargino, one can refer to Ref.[4][20]. The couplings of $Higgs(B) - \tilde{\chi}_k^+ - \tilde{\chi}_k^+$ are

$$V_{B\tilde{\chi}_k^+\tilde{\chi}_k^+} = V_{B\tilde{\chi}_k^+\tilde{\chi}_k^+}^s + V_{B\tilde{\chi}_k^+\tilde{\chi}_k^+}^{ps} \gamma_5 \quad (B = h^0, H^0, A^0, G^0), \quad (2.21.1)$$

where the notations defined above, which are involved in our calculation, are explicitly expressed as below:

$$V_{H^0 \tilde{\chi}_k^+ \tilde{\chi}_k^+}^s = \frac{-ig}{\sqrt{2}} [\cos \alpha \text{Re}(V_{k,1} U_{k,2}) + \sin \alpha \text{Re}(V_{k,2} U_{k,1})] \quad (2.21.2)$$

$$V_{h^0 \tilde{\chi}_k^+ \tilde{\chi}_k^+}^s = \frac{ig}{\sqrt{2}} [\sin \alpha \text{Re}(V_{k,1} U_{k,2}) - \cos \alpha \text{Re}(V_{k,2} U_{k,1})] \quad (2.21.3)$$

$$V_{A^0 \tilde{\chi}_k^+ \tilde{\chi}_k^+}^{ps} = \frac{g}{\sqrt{2}} [\sin \beta \text{Re}(V_{k,1} U_{k,2}) + \cos \beta \text{Re}(V_{k,2} U_{k,1})] \quad (2.21.4)$$

$$V_{G^0 \tilde{\chi}_k^+ \tilde{\chi}_k^+}^{ps} = \frac{-g}{\sqrt{2}} [\cos \beta \text{Re}(V_{k,1} U_{k,2}) - \sin \beta \text{Re}(V_{k,2} U_{k,1})] \quad (2.21.5)$$

We define the following notations in Higgs-quark-quark and Higgs-squark-squark couplings:

$$H^0 - U - U : V_{H^0 UU} = \frac{-igm_U \sin \alpha}{2m_W \sin \beta}, \quad H^0 - D - D : V_{H^0 DD} = \frac{-igm_D \cos \alpha}{2m_W \cos \beta}, \quad (2.22.1)$$

$$h^0 - U - U : V_{h^0 UU} = \frac{-igm_U \cos \alpha}{2m_W \sin \beta}, \quad h^0 - D - D : V_{h^0 DD} = \frac{igm_D \sin \alpha}{2m_W \cos \beta}, \quad (2.22.2)$$

$$A^0 - U - U : V_{A^0 UU} \gamma_5 = \frac{-gm_U \cot \beta}{2m_W} \gamma_5, \quad A^0 - D - D : V_{A^0 DD} \gamma_5 = \frac{-gm_D \tan \beta}{2m_W} \gamma_5, \quad (2.22.3)$$

$$G^0 - U - U : V_{G^0 UU} \gamma_5 = \frac{-gm_U}{2m_W} \gamma_5, \quad G^0 - D - D : V_{G^0 DD} \gamma_5 = \frac{gm_D}{2m_W} \gamma_5. \quad (2.22.4)$$

The couplings of $H^0(h^0) - \tilde{q}_i - \tilde{q}_i$ ($i = 1, 2, q = u, d, c, s, t, b$) are

$$\begin{aligned} V_{H^0 \tilde{U}_1 \tilde{U}_1} &= \frac{-igm_Z \cos(\alpha + \beta)}{\cos \theta_W} \left[\left(\frac{1}{2} - \frac{2}{3} \sin^2 \theta_W \right) \cos^2 \theta_U + \frac{2}{3} \sin^2 \theta_W \sin^2 \theta_U \right] \\ &\quad - \frac{igm_U^2 \sin \alpha}{m_W \sin \beta} + \frac{igm_U}{2m_W \sin \beta} (A_U \sin \alpha + \mu \cos \alpha) \sin \theta_U \cos \theta_U \cos 2\phi_U, \end{aligned} \quad (2.23.1)$$

$$\begin{aligned} V_{H^0 \tilde{U}_2 \tilde{U}_2} &= \frac{-igm_Z \cos(\alpha + \beta)}{\cos \theta_W} \left[\left(\frac{1}{2} - \frac{2}{3} \sin^2 \theta_W \right) \sin^2 \theta_U + \frac{2}{3} \sin^2 \theta_W \cos^2 \theta_U \right] \\ &\quad - \frac{igm_U^2 \sin \alpha}{m_W \sin \beta} - \frac{igm_U}{2m_W \sin \beta} (A_U \sin \alpha + \mu \cos \alpha) \sin \theta_U \cos \theta_U \cos 2\phi_U, \end{aligned} \quad (2.23.2)$$

$$\begin{aligned}
V_{H^0 \tilde{D}_1 \tilde{D}_1} &= \frac{igm_Z \cos(\alpha + \beta)}{\cos \theta_W} \left[\left(\frac{1}{2} - \frac{1}{3} \sin^2 \theta_W \right) \cos^2 \theta_D + \frac{1}{3} \sin^2 \theta_W \sin^2 \theta_D \right] \\
&\quad - \frac{igm_D^2 \cos \alpha}{m_W \cos \beta} + \frac{igm_D}{2m_W \cos \beta} (A_D \cos \alpha + \mu \sin \alpha) \sin \theta_D \cos \theta_D \cos 2\phi_D, \quad (2.23.3)
\end{aligned}$$

$$\begin{aligned}
V_{H^0 \tilde{D}_2 \tilde{D}_2} &= \frac{igm_Z \cos(\alpha + \beta)}{\cos \theta_W} \left[\left(\frac{1}{2} - \frac{1}{3} \sin^2 \theta_W \right) \sin^2 \theta_D + \frac{1}{3} \sin^2 \theta_W \cos^2 \theta_D \right] \\
&\quad - \frac{igm_D^2 \cos \alpha}{m_W \cos \beta} - \frac{igm_D}{2m_W \cos \beta} (A_D \cos \alpha + \mu \sin \alpha) \sin \theta_D \cos \theta_D \cos 2\phi_D, \quad (2.23.4)
\end{aligned}$$

$$\begin{aligned}
V_{h^0 \tilde{U}_1 \tilde{U}_1} &= \frac{igm_Z \sin(\alpha + \beta)}{\cos \theta_W} \left[\left(\frac{1}{2} - \frac{2}{3} \sin^2 \theta_W \right) \cos^2 \theta_U + \frac{2}{3} \sin^2 \theta_W \sin^2 \theta_U \right] \\
&\quad - \frac{igm_U^2 \cos \alpha}{m_W \sin \beta} + \frac{igm_U}{2m_W \sin \beta} (A_U \cos \alpha - \mu \sin \alpha) \sin \theta_U \cos \theta_U \cos 2\phi_U, \quad (2.23.5)
\end{aligned}$$

$$\begin{aligned}
V_{h^0 \tilde{U}_2 \tilde{U}_2} &= \frac{igm_Z \sin(\alpha + \beta)}{\cos \theta_W} \left[\left(\frac{1}{2} - \frac{2}{3} \sin^2 \theta_W \right) \sin^2 \theta_U + \frac{2}{3} \sin^2 \theta_W \cos^2 \theta_U \right] \\
&\quad - \frac{igm_U^2 \cos \alpha}{m_W \sin \beta} - \frac{igm_U}{2m_W \sin \beta} (A_U \cos \alpha - \mu \sin \alpha) \sin \theta_U \cos \theta_U \cos 2\phi_U, \quad (2.23.6)
\end{aligned}$$

$$\begin{aligned}
V_{h^0 \tilde{D}_1 \tilde{D}_1} &= \frac{-igm_Z \sin(\alpha + \beta)}{\cos \theta_W} \left[\left(\frac{1}{2} - \frac{1}{3} \sin^2 \theta_W \right) \cos^2 \theta_D + \frac{1}{3} \sin^2 \theta_W \sin^2 \theta_D \right] \\
&\quad + \frac{igm_D^2 \sin \alpha}{m_W \cos \beta} - \frac{igm_D}{2m_W \cos \beta} (A_D \sin \alpha - \mu \cos \alpha) \sin \theta_D \cos \theta_D \cos 2\phi_D, \quad (2.23.7)
\end{aligned}$$

$$\begin{aligned}
V_{h^0 \tilde{D}_2 \tilde{D}_2} &= \frac{-igm_Z \sin(\alpha + \beta)}{\cos \theta_W} \left[\left(\frac{1}{2} - \frac{1}{3} \sin^2 \theta_W \right) \sin^2 \theta_D + \frac{1}{3} \sin^2 \theta_W \cos^2 \theta_D \right] \\
&\quad + \frac{igm_D^2 \sin \alpha}{m_W \cos \beta} + \frac{igm_D}{2m_W \cos \beta} (A_D \sin \alpha - \mu \cos \alpha) \sin \theta_D \cos \theta_D \cos 2\phi_D, \quad (2.23.8)
\end{aligned}$$

respectively.

3. The calculation of subprocess $\gamma\gamma \rightarrow \tilde{\chi}_1^+ \tilde{\chi}_1^-$ in the MSSM.

Charginos are produced in the t- and u-channel with intermediate charginos at the lowest order. The Feynman diagrams for the process at the tree level are shown in Fig.1(a), where the u-channel tree-level is not drawn. The relevant Feynman rules can be found in reference[4]. The one-loop diagrams involving quarks and their supersymmetric partners for the subprocess $\gamma\gamma \rightarrow \tilde{\chi}_1^+ \tilde{\chi}_1^-$, are drawn in Fig.1 ($b \sim g$), where we only give the third generation quark and squark loop diagrams. All the one-loop diagrams can be divided into five groups: (1) $\gamma\tilde{\chi}_1^+ \tilde{\chi}_1^-$ vertex correction diagrams shown as Fig.1(b). (2) box diagrams as Fig.1(c). (3) quartic interaction diagrams as Fig.1(d). (4) triangle diagrams as Fig.1(e). (5) self-energy correction diagram as Fig.1(f). The chargino, γ and $Z^0 - \gamma$ mixing self-energy diagrams shown as Fig.1(g). The total cross section including the leading one-loop corrections in the frame of the MSSM should be

$$\hat{\sigma} = \hat{\sigma}_0 + \delta\hat{\sigma}^{1-loop},$$

where $\delta\hat{\sigma}^{1-loop}$ represents the cross section with all virtual quarks and their SUSY partners corrections. In the calculation, we use the t'Hooft gauge and adopt the dimensional reduction scheme(DR) [19], which is commonly used in the calculation of the radiative corrections in frame of the MSSM as it preserves supersymmetry at least at one-loop order, to control the ultraviolet divergences in the virtual loop corrections. We choose the on-mass-shell scheme (OMS)[21] in doing renormalization.

3.1 The tree-level formulae and notations.

In this work, we denote the reaction of chargino pair production via photon-photon

collision as:

$$\gamma(p_3, \mu)\gamma(p_4, \nu) \longrightarrow \tilde{\chi}_1^+(p_1)\tilde{\chi}_1^-(p_2). \quad (3.1.1)$$

where p_1 and p_2 represent the momenta of the outgoing chargino pair and p_3 and p_4 describe the momenta of the two incoming photons, respectively. The Mandelstam variables \hat{s} , \hat{t} and \hat{u} are defined as $\hat{s} = (p_1 + p_2)^2$, $\hat{t} = (p_1 - p_3)^2$, $\hat{u} = (p_1 - p_4)^2$. The corresponding Lorentz invariant matrix element at the lowest order for the reaction $\gamma\gamma \rightarrow \tilde{\chi}_1^+\tilde{\chi}_1^-$ is written as

$$\mathcal{M}_0 = \mathcal{M}_{\hat{t}} + \mathcal{M}_{\hat{u}}, \quad (3.1.2)$$

where

$$\mathcal{M}_{\hat{t}} = \left[\bar{u}(p_3)(-ie\gamma_\mu) \frac{i}{\hat{\not{p}} - m_{\tilde{\chi}_1^+}} (-ie\gamma_\nu)v(p_4)\epsilon^\mu(p_1)\epsilon^\nu(p_2) \right], \quad (3.1.3)$$

$$\mathcal{M}_{\hat{u}} = \left[\bar{u}(p_3)(-ie\gamma_\nu) \frac{i}{\hat{\not{p}} - m_{\tilde{\chi}_1^+}} (-ie\gamma_\mu)v(p_4)\epsilon^\nu(p_2)\epsilon^\mu(p_1) \right]. \quad (3.1.4)$$

The corresponding differential cross section is obtained by

$$\frac{d\hat{\sigma}_0(\hat{t}, \hat{s})}{d\hat{t}} = \frac{1}{16\pi^2\hat{s}} \sum_{\text{spins}} |\mathcal{M}_0|^2, \quad (3.1.5)$$

where the bar over the summation means to sum up the spins of final states and average the spins of initial photons. After integration over \hat{t} , the total Born cross section with unpolarized incoming photons is given by[24]

$$\hat{\sigma}_0(\hat{s}) = \frac{2\pi\alpha^2}{\hat{s}} \left[-2\hat{\beta}(2 - \hat{\beta}^2) + (3 - \hat{\beta}^4) \ln \frac{1 + \hat{\beta}}{1 - \hat{\beta}} \right]. \quad (3.1.6)$$

where the kinematic factor is defined as

$$\hat{\beta} = \sqrt{1 - 4m_{\tilde{\chi}_1^+}^2/\hat{s}}. \quad (3.1.7)$$

3.2 Self-energies.

The self-energies of γ and its mixing with Z^0 contributed by the one-loop diagrams of virtual quarks and squarks shown in Fig.1(g.2) read:

$$\begin{aligned}\Sigma_T^{AA}(p^2) &= \frac{N_c e^2}{8\pi^2} \sum_{q=(u,d)}^{(c,s),(t,b)} \left\{ 2Q_q^2 (m_q^2 B_0^q - p^2 B_1^q - p^2 B_{21}^q + (2-\epsilon) B_{22}^q) \right. \\ &\quad \left. + \sum_{i=1,2} \left[Q_q^2 (2B_{22}^{\tilde{q}_i} - A_0(m_{\tilde{q}_i})) \right] \right\}, \quad (3.2.1)\end{aligned}$$

$$\begin{aligned}\Sigma_T^{AZ}(p^2) &= \frac{N_c e g}{16\pi^2 c_W} \sum_{(U,D)=(u,d)}^{(c,s),(t,b)} \left\{ Q_D (\cos^2 \theta_D + 2Q_D s_W^2) (A_0(m_{\tilde{D}_1}) - (2-\epsilon) B_{22}^{\tilde{D}_1}) \right. \\ &\quad + Q_D (\sin^2 \theta_D + 2Q_D s_W^2) (A_0(m_{\tilde{D}_2}) - B_{22}^{\tilde{D}_2}) \\ &\quad - Q_D (1 + 4Q_D s_W^2) (m_D^2 B_0^D - p^2 B_1^D - p^2 B_{21}^D + (2-\epsilon) B_{22}^D) \\ &\quad \left. + (Q_D \rightarrow -Q_U, D \rightarrow U, \tilde{D} \rightarrow \tilde{U}, \theta_D \rightarrow \theta_U) \right\} \quad (3.2.2)\end{aligned}$$

where $\epsilon = 4 - d$ and d is the space-time dimension. In the two equations above, we denote $\{B_i^q, B_{ij}^q\} = \{B_i, B_{ij}\}(p, m_q, m_q)$, ($q = u, d, c, s, t, b$). θ_q 's as the mixing angles of squark sectors, respectively. Then the renormalization conditions yield the corresponding counterterms of the wave functions and the electric charge as:

$$\delta Z_{AA} = -\frac{\partial \Sigma_T^{AA}(p^2)}{\partial p^2} \Big|_{p^2=0}, \quad (3.2.3)$$

$$\delta Z_{ZA} = 2 \frac{\Sigma_T^{AZ}(0)}{m_Z^2} = 0, \quad (3.2.4)$$

$$\delta Z_e = \frac{1}{2} \frac{\partial \Sigma_T^{AA}(p^2)}{\partial p^2} \Big|_{p^2=0} - \frac{s_W}{c_W} \frac{\Sigma_T^{AZ}(0)}{m_Z^2} = -\frac{1}{2} \delta Z_{AA}. \quad (3.2.5)$$

The chargino wave function corrections $\delta Z_{\tilde{\chi}_i^+ \tilde{\chi}_i^+}$'s are determined in terms of the one-particle irreducible two-point function $i\Gamma_{ii}(p^2)$ for charginos in the DR mass basis. It should be written as[22]:

$$\Gamma_{ii}(p^2) = (\not{p} - m_t) + [\not{p} P_L \Sigma_{ii}^L(p^2) + \not{p} P_R \Sigma_{ii}^R(p^2) + P_L \Sigma_{ii}^{S,L}(p^2) + P_R \Sigma_{ii}^{S,R}(p^2)]. \quad (3.2.6)$$

With the Feynman rules of the interactions of quark-squark-chargino in Eqs.(2.18.1~4), Eqs.(2.19.1~4) and Eqs.(2.20.1~4), the corresponding unrenormalized chargino self-energies including CP violation phases read(see Fig.1(g.1))

$$\begin{aligned} \Sigma_{\tilde{\chi}_i^+ \tilde{\chi}_i^+}^{S,L}(p^2) &= \frac{-N_c}{16\pi^2} \sum_{(U,D)=(u,d)}^{(c,s),(t,b)} \sum_{k=1,2} \left\{ m_D V_{D\tilde{U}_k \tilde{\chi}_i^+}^{(1)} V_{D\tilde{U}_k \tilde{\chi}_i^+}^{(2)*} B_0[p, m_D, m_{\tilde{U}_k}] \right. \\ &\quad \left. - m_U V_{U\tilde{D}_k \tilde{\chi}_i^+}^{(1)} V_{U\tilde{D}_k \tilde{\chi}_i^+}^{(2)*} B_0[p, m_U, m_{\tilde{D}_k}] \right\}, \end{aligned} \quad (3.2.7)$$

$$\begin{aligned} \Sigma_{\tilde{\chi}_i^+ \tilde{\chi}_i^+}^{S,R}(p^2) &= \frac{-N_c}{16\pi^2} \sum_{(U,D)=(u,d)}^{(c,s),(t,b)} \sum_{k=1,2} \left\{ m_D V_{D\tilde{U}_k \tilde{\chi}_i^+}^{(2)} V_{D\tilde{U}_k \tilde{\chi}_i^+}^{(1)*} B_0[p, m_D, m_{\tilde{U}_k}] \right. \\ &\quad \left. - m_U V_{U\tilde{D}_k \tilde{\chi}_i^+}^{(2)} V_{U\tilde{D}_k \tilde{\chi}_i^+}^{(1)*} B_0[p, m_U, m_{\tilde{D}_k}] \right\}, \end{aligned} \quad (3.2.8)$$

$$\Sigma_{\tilde{\chi}_i^+ \tilde{\chi}_i^+}^L(p^2) = \frac{N_c}{16\pi^2} \sum_{(U,D)=(u,d)}^{(c,s),(t,b)} \sum_{k=1,2} \left\{ V_{D\tilde{U}_k \tilde{\chi}_i^+}^{(1)} V_{D\tilde{U}_k \tilde{\chi}_i^+}^{(1)*} B_1[p, m_D, m_{\tilde{U}_k}] - V_{U\tilde{D}_k \tilde{\chi}_i^+}^{(1)} V_{U\tilde{D}_k \tilde{\chi}_i^+}^{(1)*} B_1[p, m_U, m_{\tilde{D}_k}] \right\}, \quad (3.2.9)$$

$$\Sigma_{\tilde{\chi}_i^+ \tilde{\chi}_i^+}^R(p^2) = \frac{N_c}{16\pi^2} \sum_{(U,D)=(u,d)}^{(c,s),(t,b)} \sum_{k=1,2} \left\{ V_{D\tilde{U}_k \tilde{\chi}_i^+}^{(2)} V_{D\tilde{U}_k \tilde{\chi}_i^+}^{(2)*} B_1[p, m_D, m_{\tilde{U}_k}] - V_{U\tilde{D}_k \tilde{\chi}_i^+}^{(2)} V_{U\tilde{D}_k \tilde{\chi}_i^+}^{(2)*} B_1[p, m_U, m_{\tilde{D}_k}] \right\}, \quad (3.2.10)$$

Imposing the on-shell renormalization conditions given in Ref.[21] [22], one can obtain the renormalization constants for the renormalized $\tilde{\chi}_1^+$ self-energies as[23]:

$$\delta \Sigma_{\tilde{\chi}_1^+ \tilde{\chi}_1^+}(p^2) = C_L \not{p} P_L + C_R \not{p} P_R - C_S^- P_L - C_S^+ P_R, \quad (3.2.11)$$

From Eq.(3.2.1) \sim (3.2.5) we find that the self-energies of $\gamma\gamma$ and γZ^0 have no contribution to the relevant counterterms of the $\gamma\tilde{\chi}_1^+\tilde{\chi}_1^+$ vertex. The renormalization constant for the $\Gamma_{\gamma\tilde{\chi}_1^+\tilde{\chi}_1^+}^\mu$ vertex is written as:

$$\delta\Gamma_{\gamma\tilde{\chi}_1^+\tilde{\chi}_1^+}^\mu = -ie\gamma^\mu[C^L P_L + C^R P_R]. \quad (3.2.12)$$

where

$$\begin{aligned} C_L &= \frac{1}{2}(\delta Z_{\tilde{\chi}_i^+\tilde{\chi}_i^+}^L + \delta Z_{\tilde{\chi}_i^+\tilde{\chi}_i^+}^{L\dagger}), \\ C_R &= \frac{1}{2}(\delta Z_{\tilde{\chi}_i^+\tilde{\chi}_i^+}^R + \delta Z_{\tilde{\chi}_i^+\tilde{\chi}_i^+}^{R\dagger}), \\ C_S^- &= \frac{m_{\tilde{\chi}_i^+}}{2}(\delta Z_{\tilde{\chi}_i^+\tilde{\chi}_i^+}^L + \delta Z_{\tilde{\chi}_i^+\tilde{\chi}_i^+}^{R\dagger}) + \delta m_{\tilde{\chi}_i^+}, \\ C_S^+ &= \frac{m_{\tilde{\chi}_i^+}}{2}(\delta Z_{\tilde{\chi}_i^+\tilde{\chi}_i^+}^R + \delta Z_{\tilde{\chi}_i^+\tilde{\chi}_i^+}^{L\dagger}) + \delta m_{\tilde{\chi}_i^+}. \end{aligned} \quad (3.2.13)$$

$$\delta m_{\tilde{\chi}_i^+} = \frac{1}{2}\tilde{R}e \left[m_{\tilde{\chi}_i^+} \Sigma_{\tilde{\chi}_i^+\tilde{\chi}_i^+}^L(m_{\tilde{\chi}_i^+}^2) + m_{\tilde{\chi}_i^+} \Sigma_{\tilde{\chi}_i^+\tilde{\chi}_i^+}^R(m_{\tilde{\chi}_i^+}^2) + \Sigma_{\tilde{\chi}_i^+\tilde{\chi}_i^+}^{S,L}(m_{\tilde{\chi}_i^+}^2) + \Sigma_{\tilde{\chi}_i^+\tilde{\chi}_i^+}^{S,R}(m_{\tilde{\chi}_i^+}^2) \right], \quad (3.2.14)$$

$$\begin{aligned} \delta Z_{\tilde{\chi}_i^+\tilde{\chi}_i^+}^L &= -\tilde{R}e \Sigma_{\tilde{\chi}_i^+\tilde{\chi}_i^+}^L(m_{\tilde{\chi}_i^+}^2) - \frac{1}{m_{\tilde{\chi}_i^+}} \tilde{R}e \left[\Sigma_{\tilde{\chi}_i^+\tilde{\chi}_i^+}^{S,R}(m_{\tilde{\chi}_i^+}^2) - \Sigma_{\tilde{\chi}_i^+\tilde{\chi}_i^+}^{S,L}(m_{\tilde{\chi}_i^+}^2) \right] \\ &- m_{\tilde{\chi}_i^+} \frac{\partial}{\partial p^2} \tilde{R}e \left\{ m_{\tilde{\chi}_i^+} \Sigma_{\tilde{\chi}_i^+\tilde{\chi}_i^+}^L(p^2) + m_{\tilde{\chi}_i^+} \Sigma_{\tilde{\chi}_i^+\tilde{\chi}_i^+}^R(p^2) \right. \\ &+ \left. \Sigma_{\tilde{\chi}_i^+\tilde{\chi}_i^+}^{S,L}(p^2) + \Sigma_{\tilde{\chi}_i^+\tilde{\chi}_i^+}^{S,R}(p^2) \right\} \Big|_{p^2=m_{\tilde{\chi}_i^+}^2}, \end{aligned} \quad (3.2.15)$$

$$\begin{aligned} \delta Z_{\tilde{\chi}_i^+\tilde{\chi}_i^+}^R &= -\tilde{R}e \Sigma_{\tilde{\chi}_i^+\tilde{\chi}_i^+}^R(m_{\tilde{\chi}_i^+}^2) - m_{\tilde{\chi}_i^+} \frac{\partial}{\partial p^2} \tilde{R}e \left\{ m_{\tilde{\chi}_i^+} \Sigma_{\tilde{\chi}_i^+\tilde{\chi}_i^+}^L(p^2) + m_{\tilde{\chi}_i^+} \Sigma_{\tilde{\chi}_i^+\tilde{\chi}_i^+}^R(p^2) \right. \\ &+ \left. \Sigma_{\tilde{\chi}_i^+\tilde{\chi}_i^+}^{S,L}(p^2) + \Sigma_{\tilde{\chi}_i^+\tilde{\chi}_i^+}^{S,R}(p^2) \right\} \Big|_{p^2=m_{\tilde{\chi}_i^+}^2}, \end{aligned} \quad (3.2.16)$$

where $\tilde{R}e$ takes the real part of the loop integrals. It ensures the reality of the renormalized Lagrangian.

3.3 Renormalized one-loop corrections.

The renormalized one-loop matrix element involves the contributions from all the one-loop vertex, box, triangle, quartic and self-energy interaction diagrams (shown in Fig.1) and their relevant counterterms. We can neglect some of the s-channel Feynman diagrams shown in Fig.1(e.2), in which each one involves a quark loop with the exchanging of γ or Z^0 boson. This is the consequence of Furry theorem, since the Furry theorem forbids the production of the spin-one components of the Z^0 and γ , and the contribution from the spin-zero component of the Z^0 vector boson coupling with a pair of chargino is very small and can be neglected. The calculation also shows the γ and Z^0 exchanging s-channel diagrams in Fig.1(d.2) and Fig.1(e.1) with a squark loop have no contribution to cross section. The contribution from each of the γ and Z^0 exchanging s-channel diagrams in Fig.1(e.1) is canceled out by the corresponding one with exchanging incoming photons. Considering only the form factors in matrix element which contribute to the total cross section, the renormalized amplitude $\delta\mathcal{M}_{1-loop}$ can be written in the following form according to their Lorentz invariant structure:

$$\begin{aligned}
\delta\mathcal{M}_{1-loop} &= \mathcal{M}^v + \mathcal{M}^b + \mathcal{M}^{tr} + \mathcal{M}^q + \mathcal{M}^s \\
&= \mathcal{M}^{v,\hat{t}} + \mathcal{M}^{v,\hat{u}} + \mathcal{M}^{b,\hat{t}} + \mathcal{M}^{b,\hat{u}} + \mathcal{M}^{tr,\hat{t}} + \mathcal{M}^{tr,\hat{u}} + \mathcal{M}^q + \mathcal{M}^{s,\hat{t}} + \mathcal{M}^{s,\hat{u}} \\
&= N_c \epsilon^\mu(p_3) \epsilon^\nu(p_4) \bar{u}(p_1) \{ f_1 \gamma_\mu \gamma_\nu + f_2 \gamma_\nu \gamma_\mu + f_3 \gamma_\mu p_{1\nu} + f_4 \gamma_\mu p_{2\nu} \\
&\quad + f_5 \gamma_\nu p_{1\mu} + f_6 \gamma_\nu p_{2\mu} + f_7 p_{1\mu} p_{1\nu} + f_8 p_{1\mu} p_{2\nu} + f_9 p_{1\nu} p_{2\mu} \\
&\quad + f_{10} p_{2\mu} p_{2\nu} + f_{11} \not{p}_3 \gamma_\mu \gamma_\nu + f_{12} \not{p}_3 \gamma_\nu \gamma_\mu + f_{13} \not{p}_3 \gamma_\mu p_{1\nu} + f_{14} \not{p}_3 \gamma_\mu p_{2\nu} \\
&\quad + f_{15} \not{p}_3 \gamma_\nu p_{1\mu} + f_{16} \not{p}_3 \gamma_\nu p_{2\mu} + f_{17} \not{p}_3 p_{1\mu} p_{1\nu} + f_{18} \not{p}_3 p_{1\mu} p_{2\nu} \\
&\quad + f_{19} \not{p}_3 p_{1\nu} p_{2\mu} + f_{20} \not{p}_3 p_{2\mu} p_{2\nu} + f_{21} \gamma_5 \epsilon_{\mu\nu\alpha\beta} p_1^\alpha p_3^\beta \}
\end{aligned}$$

$$+ f_{22}\gamma_5\epsilon_{\mu\nu\alpha\beta}p_2^\alpha p_3^\beta\} v(p_2), \quad (3.3.1)$$

with

$$f_i = f_i^v + f_i^b + f_i^{tr} + f_i^q + f_i^s \quad (i = 1 \sim 22), \quad (3.3.2)$$

where \mathcal{M}^v , \mathcal{M}^b , \mathcal{M}^{tr} , \mathcal{M}^q and \mathcal{M}^s are the renormalized matrix elements contributed by vertex, box, triangle, quartic interaction and self-energy corrections, respectively. f_i^v , f_i^b , f_i^{tr} , f_i^q and f_i^s are the corresponding form factors. We divide the matrix elements \mathcal{M}^v , \mathcal{M}^b , \mathcal{M}^{tr} and \mathcal{M}^s into t- and u-channel parts, respectively. For each of the corresponding form factor we have

$$f_i^v = f_i^{v,\hat{t}} + f_i^{v,\hat{u}}, \quad f_i^b = f_i^{b,\hat{t}} + f_i^{b,\hat{u}}, \quad f_i^{tr} = f_i^{tr,\hat{t}} + f_i^{tr,\hat{u}}, \quad f_i^s = f_i^{s,\hat{t}} + f_i^{s,\hat{u}}. \quad (i = 1 \sim 22),$$

Since the amplitude parts from the u-channel vertex, box and quartic interaction corrections can be obtained from the t-channel's by doing exchange as below:

$$\mathcal{M}^{j,\hat{u}} = \mathcal{M}^{j,\hat{t}}(t \rightarrow u, p_3 \leftrightarrow p_4, \mu \leftrightarrow \nu), \quad (j = v, b, tr, s)$$

we list only the explicit t-channel form factors $f_i^{v,\hat{t}}$, $f_i^{b,\hat{t}}$ and $f_i^{tr,\hat{t}}$ ($i = 1 \sim 22$) in Appendix. Then we can arrive at the (s)quarks one-loop corrections of the cross section for this subprocess in unpolarized photon collisions.

$$\delta\hat{\sigma}^{1-loop}(\hat{s}) = \frac{1}{16\pi\hat{s}^2} \int_{\hat{t}^-}^{\hat{t}^+} d\hat{t} \, 2Re \sum_{spins}^- \left(\mathcal{M}_0^\dagger \cdot \delta\mathcal{M}_{1-loop} \right), \quad (3.3.3)$$

where $\hat{t}^\pm = (m_{\chi_1}^2 - \frac{1}{2}\hat{s}) \pm \frac{1}{2}\hat{s}\beta$. The bar over the sum means that we are taking average over initial spins.

In our calculation, some parts of self-energies and vertex corrections are similar with those in [10][?]. The comparison with their expressions have been performed. We find that our self-energy of chargino agrees with the expressions in References [10] and [12] when there is no CP-violation phases, but the self-energies of γ and $\gamma - Z^0$ mixing from quark loops presented above have discrepancies with equations (C.11) and (C.13) in Ref.[10]. The self-energy parts from quark loop in Eqs.(3.2.1) and (3.2.2) in our paper are coincident with the expressions for the SM[17].

4. Numerical results and discussions

In the following numerical evaluation, we present some results of the one-loop radiative corrections of virtual (s)quarks to the cross sections of the lightest chargino pair production in the processes of $\gamma\gamma \rightarrow \tilde{\chi}_1^+ \tilde{\chi}_1^-$ and $e^+e^- \rightarrow \gamma\gamma \rightarrow \tilde{\chi}_1^+ \tilde{\chi}_1^-$, respectively. The input parameters on the MSSM can be divided into two parts. One is for the SM parameters and the other is for SUSY parameters. The SM parameters are chosen as: $m_t = 175 \text{ GeV}$, $m_Z = 91.187 \text{ GeV}$, $m_b = 4.5 \text{ GeV}$, $\sin^2 \theta_W = 0.2315$, and $\alpha = 1/137.036$. The SUSY parameters are taken as follows by default unless otherwise stated.

(1) The masses of squark mass eigenstates $\tilde{U}_{1,2}$ ($\tilde{U} = \tilde{u}, \tilde{c}, \tilde{t}$) and $\tilde{D}_{1,2}$ ($\tilde{D} = \tilde{d}, \tilde{s}, \tilde{b}$) are determined by Eqs.(2.2 ~ 2.10). From renormalization group equations [18] one expects that the soft SUSY breaking masses $m_{\tilde{q}_L}$ and $m_{\tilde{q}_R}$ of the third generation squarks are smaller than those of the first and second generations due to the Yukawa interactions. The mixing between the left- and right-handed stop quarks \tilde{t}_L and \tilde{t}_R can be very large due to the large

mass of the top quark, and the lightest scalar top quark mass eigenstate \tilde{t}_1 can be much lighter than the top mass and all the scalar partners of the light quarks. Here the left-right mixing of the top squark plays an important role. We assume $m_{\tilde{U}_1} < m_{\tilde{U}_2}$, $m_{\tilde{D}_1} < m_{\tilde{D}_2}$ and for simplicity we take the stop and sbottom mixing angles being the values of $\theta_t = \frac{\pi}{4}$ and $\theta_b = 0$, respectively, but the mixing angles of the first and second generation squarks are set to be $\tan \theta_{u,d,c,s} = 0.2$. In numerical calculation, we take $\tilde{M}_Q = \tilde{M}_U = \tilde{M}_D = \tilde{M} = 200 \text{ GeV}$ (for the third generation) and 600 GeV (for the first and second generations). The ratio of the vacuum expectation values $\tan \beta$ is set to be 4 or 40 in order to make comparison.

(2) The neutral Higgs boson masses m_{h^0} , m_{H^0} and m_{A^0} are given by[26]

$$m_{h^0, H^0}^2 = \frac{1}{2} \left[m_{A^0}^2 + m_Z^2 + \epsilon \mp \sqrt{(m_{A^0}^2 + m_Z^2 + \epsilon)^2 - 4m_{A^0}^2 m_Z^2 \cos^2 2\beta - 4\epsilon(m_{A^0}^2 \sin^2 \beta + m_Z^2 \cos^2 \beta)} \right], \quad (4.1)$$

$$m_{H^\pm}^2 = m_{A^0}^2 + m_W^2 \quad (4.2)$$

with the leading corrections being characterized by the radiative parameter ϵ

$$\epsilon = \frac{3G_F}{\sqrt{2}\pi^2} \frac{m_t^4}{\sin^2 \beta} \log \left[\frac{m_{\tilde{t}}^2}{m_t^2} \right]. \quad (4.3)$$

The parameter $m_{\tilde{t}}^2 = m_{\tilde{t}_1} m_{\tilde{t}_2}$ denotes the average squared mass of the stop quarks. The mixing angle α is fixed by $\tan \beta$ and the Higgs boson mass m_{A^0} ,

$$\tan 2\alpha = \tan 2\beta \frac{m_{A^0}^2 + m_Z^2}{m_{A^0}^2 - m_Z^2 + \frac{\epsilon}{\cos 2\beta}} \quad \left(-\frac{\pi}{2} < \alpha < 0 \right). \quad (4.4)$$

In this paper, we take $m_{A^0} = 150 \text{ GeV}$.

(3) The physical chargino masses $m_{\tilde{\chi}_1^+}$ and $m_{\tilde{\chi}_2^+}$ are set to be 165 GeV and 750 GeV, respectively. Assuming that μ has positive sign, the fundamental SUSY parameters $M_{SU(2)}$ and $|\mu|$ can be extracted at the tree level from these input chargino masses, $\tan\beta$ and the complex phase angle of μ by using Eqs.(2.15). When the lightest chargino is dominantly gaugino (gaugino-like or wino-like), we should have $M_{SU(2)} \ll |\mu|$ from Eq.(2.15), and when the chargino is dominantly Higgsino (Higgsino-like), $M_{SU(2)}$ should be much larger than $|\mu|$. Here we define the relative corrections for subprocess $\gamma\gamma \rightarrow \tilde{\chi}_1^+ \tilde{\chi}_1^-$ and process $e^+e^- \rightarrow \gamma\gamma \rightarrow \tilde{\chi}_1^+ \tilde{\chi}_1^-$ as

$$\hat{\delta} = \frac{\delta\hat{\sigma}^{1-loop}}{\hat{\sigma}_0}, \quad \delta = \frac{\delta\sigma^{1-loop}}{\sigma_0}, \quad (4.5)$$

respectively. The relative corrections of all the quarks and their SUSY partners as the functions of the c.m.s. energy of photons $\sqrt{\hat{s}}$ with $m_{\tilde{\chi}_1^+} = 165 \text{ GeV}$, $m_{\tilde{\chi}_2^+} = 750 \text{ GeV}$ and all CP phases being zero, are shown in Fig.3(a) and (b). In figure 3(a) the two curves correspond to the Higgsino-like and gaugino-like chargino pair productions with $\tan\beta = 4$, respectively, while the plot in Figure 3(b) is for both Higgsino-like and gaugino-like chargino cases with $\tan\beta = 40$. In general, the corrections with $\tan\beta = 40$ are approximately twice as large as those with $\tan\beta = 4$. Because of the resonance effects, all the four curves in Fig.3(a) \sim (b) have peaks or spikes at the energy positions where the resonance conditions are satisfied. The large enhancement peaks on all four curves are located in the vicinity of $\sqrt{\hat{s}} = 2m_t = 350 \text{ GeV}$. On the two curves of Fig.3(a) with $\tan\beta = 4$, there are two small spikes stemming from resonance effects in the vicinities of $\sqrt{\hat{s}} \sim 2m_{\tilde{b}_{1,2}} \sim 403 \text{ GeV}$ and $\sqrt{\hat{s}} = 2m_{\tilde{t}_2} \sim 674 \text{ GeV}$, whereas for the two curves in Fig.3(b) with $\tan\beta = 40$, the small

spikes due to resonance effect are located at the positions of $\sqrt{\hat{s}} \sim 2m_{\tilde{b}_{1,2}} \sim 400 \text{ GeV}$ and $\sqrt{\hat{s}} = 2m_{\tilde{t}_2} \sim 690 \text{ GeV}$, respectively. Figure 4 gives the relative corrections of the subprocess as a function of self-supersymmetry-breaking mass parameter of the third generation scalar quarks \tilde{M} (We set the \tilde{M} for the first and second generations being 600 GeV.) with $\sqrt{\hat{s}} = 400 \text{ GeV}$ and all three CP-odd phases being zero. In this figure we can see considerable enhancement around the points of $\tilde{M} = 205 \text{ GeV}$ for $\tan\beta = 4$ and $\tilde{M} = 219 \text{ GeV}$ for $\tan\beta = 40$, due to the influence of the singularity in the lightest chargino wave function renormalization. This singularity originates from the renormalization constants $\delta Z_{\tilde{\chi}_1^+ \tilde{\chi}_1^+}^L$ and $\delta Z_{\tilde{\chi}_1^+ \tilde{\chi}_1^+}^R$ of the lightest chargino wave function (see Eq.(3.2.9) and Eq.(3.2.10)) at the point in parameter space where $m_{\tilde{\chi}_1^+} = m_{\tilde{t}_1} + m_b$. And in the vicinities of $\tilde{M} \sim 235 \text{ GeV}$ (for $\tan\beta = 4$ curves) and $\tilde{M} \sim 250 \text{ GeV}$ (for $\tan\beta = 40$ curves), there is a small suppression spike which shows the resonance effect on each curve, where $\sqrt{\hat{s}} = 400 \text{ GeV} \approx 2m_{\tilde{t}_1}$. We can also see that in the Higgsino-like case the relative corrections for $\tan\beta = 40$ are generally larger than those for $\tan\beta = 4$, but in gaugino-like case the dependence of the correction on the $\tan\beta$ is not so clear except in the vicinity of the singularity region. All the four curves show that the relative corrections have weak dependence on \tilde{M} except in some special regions.

The relative correction of the subprocess cross section versus the lightest chargino mass $m_{\tilde{\chi}_1^+}$ with $\sqrt{\hat{s}} = 400 \text{ GeV}$ and $\phi_\mu = \phi_t = \phi_b = 0$, are depicted in figure 5. The four curves show obvious correction enhancement at the positions of $m_{\tilde{\chi}_1^+} = 160 \text{ GeV}$ for $\tan\beta = 4$ and $m_{\tilde{\chi}_1^+} = 139 \text{ GeV}$ for $\tan\beta = 40$, respectively. This is once again the effect of the singularity due to the renormalization constants in the lightest chargino wave function when

$$m_{\tilde{\chi}_1^+} = m_{\tilde{t}_1} + m_b.$$

The relative corrections in the subprocess of Higgsino-like chargino pair production versus the CP phases angles $\phi_{CP}(\phi_\mu, \phi_{t,b})$ with $\sqrt{\hat{s}} = 400 \text{ GeV}$, $m_{\tilde{\chi}_1^+} = 165 \text{ GeV}$ and $m_{\tilde{\chi}_2^+} = 750 \text{ GeV}$, are depicted in figure 6. The full-line and dotted-line correspond to $\phi_{CP} = \phi_t = \phi_b$ with $\tan\beta = 4$ and $\tan\beta = 40$, respectively. The dashed-line and dash-and-dotted-line correspond to $\phi_{CP} = \phi_\mu$ with $\tan\beta = 4$ and $\tan\beta = 40$, respectively. Fig.6 shows the periodical features of $\hat{\delta}(\phi_t) = \hat{\delta}(\pi + \phi_t)$ for the curves of $\hat{\delta}$ versus ϕ_t and $\hat{\delta}(\phi_\mu) = \hat{\delta}(2\pi + \phi_\mu)$ for the curves of $\hat{\delta}$ versus ϕ_μ , respectively. All the three CP phase angles affect the corrections obviously.

From our numerical calculation with the parameters chosen above, we find in the Higgsino-like chargino pair production the radiative corrections from the first and second generation quarks and squarks are only few millesimal of the total corrections for our choice of parameters. The corrections are mainly from the loop diagrams of top, bottom quarks and their supersymmetric partners. But in the gaugino-like case, the radiative corrections from the first and second generation quarks and squarks can reach 3 percent of the total contribution.

The chargino pair production via photon-photon fusion is only a subprocess of the parent e^+e^- linear collider. It is easy to obtain the total cross section of the lightest chargino pair production via photon fusion in e^+e^- collider, by folding the cross section of the subprocess $\hat{\sigma}(\gamma\gamma \rightarrow \tilde{\chi}_1^+ \tilde{\chi}_1^-)$ with the photon luminosity.

$$\sigma(s) = \int_{2m_{\tilde{t}_1}/\sqrt{s}}^{x_{max}} dz \frac{dL_{\gamma\gamma}}{dz} \hat{\sigma}(\gamma\gamma \rightarrow \tilde{\chi}_1^+ \tilde{\chi}_1^- \text{ at } \hat{s} = z^2 s), \quad (4.6)$$

where \sqrt{s} and $\sqrt{\hat{s}}$ are the e^+e^- and $\gamma\gamma$ c.m.s. energies respectively and $dL_{\gamma\gamma}/dz$ is the

distribution function of photon luminosity, which is

$$\frac{dL_{\gamma\gamma}}{dz} = 2z \int_{z^2/x_{max}}^{x_{max}} \frac{dx}{x} f_{\gamma/e}(x) f_{\gamma/e}(z^2/x), \quad (4.7)$$

where $f_{\gamma/e}$ is the photon structure function of the electron beam [27, 28]. We take the structure function of the photon produced by Compton backscattering as [27, 29]

$$f_{\gamma/e}^{Comp} = \begin{cases} \frac{1}{1.8397} \left(1 - x + \frac{1}{1-x} - \frac{4x}{x_i(1-x)} + \frac{4x^2}{x_i^2(1-x)^2} \right), & \text{for } x < 0.83, x_i = 2(1 + \sqrt{2}) \\ 0, & \text{for } x > 0.83. \end{cases} \quad (4.8)$$

The cross section including all (s)quark loop corrections for the process of the lightest Higgsino-like chargino pair production $e^+e^- \rightarrow \gamma\gamma \rightarrow \tilde{\chi}_1^+ \tilde{\chi}_1^-$ versus \sqrt{s} , with $m_{\tilde{\chi}_1^+} = 165 \text{ GeV}$, $m_{\tilde{\chi}_2^+} = 750 \text{ GeV}$ and all of CP phases being zero, are depicted in Fig.7(a). Their relative corrections δ versus \sqrt{s} are presented in Fig.7(b). By analysing our numerical data, we can see the value of the relative correction δ can approach 3.2% in Higgsino-like chargino pair production, when \sqrt{s} is 0.5 TeV, $\tan\beta = 40$ and all CP phase angles are set to zero. Fig.7(a) shows that the cross section of the Higgsino-like chargino pair production via photon-photon collision in the NLC can be over one pico-bar. In Fig.7(b) we can see that the relative corrections have very weak dependence on the c.m.s energy \sqrt{s} both for the Higgsino-like and gaugino-like chargino cases, when the c.m.s energy \sqrt{s} is beyond 900 GeV.

After comparing our numerical results with those in References [12] and [10] which deal with the chargino pair production via e^+e^- collision, we find the numerical order of the corrections in this paper approach the former [12] instead of the latter [10], though the

processes investigated are different. Moreover, Our calculation shows that the contributions from (s)quark loops from all the three generations should be considered, though generally the contribution from the third generation dominates, but in gaugino-like chargino case the contributions of the first two generations cannot be neglected in precise calculation.

5. Summary

In this paper, we have analysed the virtual one-loop corrections of all the (s)quarks within the MSSM to the lightest chargino pair production at the future NLC operating in photon-photon collision mode. From the results of numerical evaluation for several typical parameter sets, it shows that the radiative corrections arising from all virtual quarks and their supersymmetric partners enhance the cross sections significantly, especially in the Higgsino-like chargino pair production process. The corrections parts contributed from the first and second generation (s)quarks are few millesimal of the total for Higgsino-like case and less than 3% for gaugino-like case, respectively. Typically, the Born cross sections for subprocess are enhanced by about one or two percent in Higgsino-like chargino case, but less than 1% in gaugino-like chargino case. In some exceptional c.m.s energy regions, where the resonance conditions are satisfied or the singularity point of the wave function renormalization constants of $\tilde{\chi}_1^+$ exists in the parameter space, the relative corrections may be observably enhanced even by three or four percent. We also investigate the effects of complex phases $\phi_{t,b}$ in the squark mass matrices and ϕ_μ appearing in chargino mass matrix in Higgsino-like case. We find the radiative corrections are very sensitive to the CP-odd complex phases ϕ_μ and $\phi_{t,b}$.

Since the lightest chargino mass, its pair production cross section and radiative corrections in both subprocess and parent process, are all strongly related to the CP-odd complex phase ϕ_μ , the experimental determination of the parameters ϕ_μ and $\phi_{t,b}$ is crucial in searching for SUSY signals.

Acknowledgement: These work was supported in part by the National Natural Science Foundation of China(project numbers: 19675033, 19875049), the Youth Science Foundation of the University of Science and Technology of China and a grant from the State Commission of Science and Technology of China.

Appendix

In this appendix we list only the form factors for the third generation quarks and squarks, and in fact we should take the sum of the form factors of the three generations for the total form factors. Some of the results have been cross-checked and they fit well with other literature such as Ref. [10].

In the following, we use the notations defined as below.

$$\begin{aligned}\bar{B}_0^{(1,k)} &= B_0[-p_1 - p_2, m_{\tilde{t}_k}, m_{\tilde{t}_k}] - \Delta, \quad \bar{B}_0^{(2,k)} = \bar{B}_0^{(1,k)}(m_{\tilde{t}_k} \rightarrow m_{\tilde{b}_k}), \\ B_0^{(3,k)}, B_1^{(3,k)} &= B_0, B_1[p_1 - p_3, m_b, m_{\tilde{t}_k}], \quad B_0^{(4,k)}, B_1^{(4,k)} = B_0, B_1[p_3 - p_1, m_t, m_{\tilde{b}_k}], \\ C_0^{(1,k)}, C_{ij}^{(1,k)} &= C_0, C_{ij}[p_1, -p_1 - p_2, m_b, m_{\tilde{t}_k}, m_{\tilde{t}_k}], \\ C_0^{(2,k)}, C_{ij}^{(2,k)} &= C_0^{(5,k)}, C_{ij}^{(5,k)}[m_b, m_{\tilde{t}_k} \rightarrow m_t, m_{\tilde{b}_k}].\end{aligned}$$

$$C_0^{(3,k)}, C_{ij}^{(3,k)} = C_0, C_{ij}[p_3, -p_1 - p_2, m_{\tilde{t}_k}, m_{\tilde{t}_k}, m_{\tilde{t}_k}].$$

$$C_0^{(4,k)}, C_{ij}^{(4,k)} = C_0^{(3,k)}, C_{ij}^{(3,k)}(p_1, p_2, p_3, m_{\tilde{t}_k} \rightarrow -p_1, -p_2, -p_3, m_{\tilde{b}_k}).$$

$$C_0^{(5)}, C_{ij}^{(5)} = C_0, C_{ij}[-p_3, p_1 + p_2, m_b, m_b, m_b], \quad C_0^{(6)}, C_{ij}^{(6)} = C_0^{(5)}, C_{ij}^{(5)}(m_b \rightarrow m_t).$$

$$C_0^{(7,k)}, C_{ij}^{(7,k)} = C_0, C_{ij}[-k_1, k_1 + k_2, m_t, m_{\tilde{b}_k}, m_{\tilde{b}_k}],$$

$$C_0^{(8,k)}, C_{ij}^{(8,k)} = C_0, C_{ij}[k_1, -k_1 - k_2, m_b, m_{\tilde{t}_k}, m_{\tilde{t}_k}],$$

$$C_0^{(9,k)}, C_{ij}^{(9,k)} = C_0, C_{ij}[k_1, -k_1 - k_2, m_{\tilde{b}_k}, m_t, m_t],$$

$$C_0^{(10,k)}, C_{ij}^{(10,k)} = C_0, C_{ij}[-k_1, k_1 + k_2, m_{\tilde{t}_k}, m_b, m_b].$$

$$D_0^{(1,k)}, D_{ij}^{(1,k)}, D_{ijl}^{(1,k)} = D_0, D_{ij}, D_{ijl}[-p_1, p_3, p_4, m_{\tilde{t}_k}, m_b, m_b, m_b]$$

$$D_0^{(2,k)}, D_{ij}^{(2,k)}, D_{ijl}^{(2,k)} = D_0, D_{ij}, D_{ijl}[p_1, -p_3, -p_4, m_{\tilde{b}_k}, m_t, m_t, m_t]$$

$$D_0^{(3,k)}, D_{ij}^{(3,k)}, D_{ijl}^{(3,k)} = D_0, D_{ij}, D_{ijl}[p_1, -p_3, -p_4, m_b, m_{\tilde{t}_k}, m_{\tilde{t}_k}, m_{\tilde{t}_k}]$$

$$D_0^{(4,k)}, D_{ij}^{(4,k)}, D_{ijl}^{(4,k)} = D_0, D_{ij}, D_{ijl}[-p_1, p_3, p_4, m_t, m_{\tilde{b}_k}, m_{\tilde{b}_k}, m_{\tilde{b}_k}]$$

$$D_0^{(5,k)}, D_{ij}^{(5,k)}, D_{ijl}^{(5,k)} = D_0, D_{ij}, D_{ijl}[p_1, -p_3, p_2, m_b, m_{\tilde{t}_k}, m_{\tilde{t}_k}, m_b]$$

$$D_0^{(6,k)}, D_{ij}^{(6,k)}, D_{ijl}^{(6,k)} = D_0, D_{ij}, D_{ijl}[-p_1, p_3, -p_2, m_t, m_{\tilde{b}_k}, m_{\tilde{b}_k}, m_t]$$

We defined some factors as below:

$$A_t = \frac{i}{\hat{t} - m_{\tilde{\chi}_1^+}^2}, \quad A_u = \frac{i}{\hat{u} - m_{\tilde{\chi}_1^+}^2},$$

$$A_h = \frac{i}{\hat{s} - m_h^2}, \quad A_H = \frac{i}{\hat{s} - m_H^2}.$$

$$A_A = \frac{i}{\hat{s} - m_A^2}, \quad A_G = \frac{i}{\hat{s} - m_Z^2}.$$

$$F_1^{q\tilde{q}'_k\tilde{\chi}_1^+} = |V_{q\tilde{q}'_k\tilde{\chi}_1^+}^{(1)}|^2 + |V_{q\tilde{q}'_k\tilde{\chi}_1^+}^{(2)}|^2, \quad F_2^{q\tilde{q}'_k\tilde{\chi}_1^+} = V_{q\tilde{q}'_k\tilde{\chi}_1^+}^{(1)*} V_{q\tilde{q}'_k\tilde{\chi}_1^+}^{(2)} + V_{q\tilde{q}'_k\tilde{\chi}_1^+}^{(2)*} V_{q\tilde{q}'_k\tilde{\chi}_1^+}^{(1)}.$$

where $q\tilde{q}'_k\tilde{\chi}_1^+ = \tilde{t}b_k\tilde{\chi}_1^+, \tilde{b}t_k\tilde{\chi}_1^+$. In the following, the expression denoted as $(t \rightarrow b)$ means replacements of $Q_t \rightarrow Q_b$, $m_t \rightarrow m_b$ and $F_i^{t\tilde{b}_k\tilde{\chi}_1^+} \rightarrow F_i^{b\tilde{t}_k\tilde{\chi}_1^+}$ ($i = 1 \sim 2$).

The one-particle-irreducible(1PI) correction to the vertex of $\gamma\tilde{\chi}_1^+\tilde{\chi}_1^+$ from quarks and their SUSY partners, can be written in terms of form factors.

$$\begin{aligned} \Delta\Gamma_{\gamma\tilde{\chi}_1^+\tilde{\chi}_1^+}^\mu(k_1, k_2) = & g_1(k_1, k_2)k_1^\mu\gamma_5\not{k}_1 + g_2(k_1, k_2)k_2^\mu\gamma_5\not{k}_1 + g_3(k_1, k_2)k_1^\mu\gamma_5\not{k}_2 \\ & + g_4(k_1, k_2)k_2^\mu\gamma_5\not{k}_2 + g_5(k_1, k_2)k_1^\mu\gamma_5 + g_6(k_1, k_2)k_2^\mu\gamma_5 \\ & + g_7(k_1, k_2)\gamma_5\gamma^\mu\not{k}_1\not{k}_2 + g_8(k_1, k_2)\gamma_5\gamma^\mu\not{k}_1 + g_9(k_1, k_2)\gamma_5\gamma^\mu\not{k}_2 \\ & + g_{10}(k_1, k_2)\gamma_5\gamma^\mu + g_{11}(k_1, k_2)k_1^\mu\not{k}_1 + g_{12}(k_1, k_2)k_2^\mu\not{k}_1 \\ & + g_{13}(k_1, k_2)k_1^\mu\not{k}_2 + g_{14}(k_1, k_2)k_2^\mu\not{k}_2 + g_{15}(k_1, k_2)k_1^\mu \\ & + g_{16}(k_1, k_2)k_2^\mu + g_{17}(k_1, k_2)\gamma^\mu\not{k}_1\not{k}_2 + g_{18}(k_1, k_2)\gamma^\mu\not{k}_1 \\ & + g_{19}(k_1, k_2)\gamma^\mu\not{k}_2 + g_{20}(k_1, k_2)\gamma^\mu, \end{aligned}$$

where k_1 and k_2 are the four-momenta of the lightest chargino pair and in their out going directions, respectively. In the equation above, the form factors of the Lorentz invariant structures including γ_5 do not contribute to the cross sections of our subprocess. Therefore we shall list only the explicit expressions of the form factors g_i ($i = 11 \sim 20$). The form factors g_i ($i = 11 \sim 20$) are expressed explicitly as follows.

$$g_{11}(k_1, k_2) = \frac{-ie}{32\pi^2} \sum_{k=1,2} \left\{ F_1^{t\tilde{b}_k\tilde{\chi}_1^+} \left[Q_b(C_{11}^{(7,k)} - C_{12}^{(7,k)} + 2C_{21}^{(7,k)} + 2C_{22}^{(7,k)} - 4C_{23}^{(7,k)}) \right] \right.$$

$$\begin{aligned}
& + 2Q_t(C_{11}^{(9,k)} - C_{12}^{(9,k)} + C_{21}^{(9,k)} + C_{22}^{(9,k)} - 2C_{23}^{(9,k)})] \\
& + (t, b, C^{(7)}, C^{(9)} \rightarrow b, t, C^{(8)}, C^{(10)})\},
\end{aligned}$$

$$\begin{aligned}
g_{12}(k_1, k_2) &= \frac{ie}{32\pi^2} \sum_{k=1,2} \left\{ F_1^{t\bar{b}_k\bar{\chi}_1^+} \left[Q_b(C_{11}^{(7,k)} - C_{12}^{(7,k)} - 2C_{22}^{(7,k)} + 2C_{23}^{(7,k)}) - 2Q_t(C_{22}^{(9,k)} - C_{23}^{(9,k)}) \right] \right. \\
& + (t, b, C^{(7)}, C^{(9)} \rightarrow b, t, C^{(8)}, C^{(10)})\},
\end{aligned}$$

$$\begin{aligned}
g_{13}(k_1, k_2) &= \frac{ie}{32\pi^2} \sum_{k=1,2} \left\{ F_1^{t\bar{b}_k\bar{\chi}_1^+} \left[Q_b(C_{12}^{(7,k)} - 2C_{22}^{(7,k)} + 2C_{23}^{(7,k)}) \right] \right. \\
& + 2Q_t(C_0^{(9,k)} + C_{11}^{(9,k)} - C_{22}^{(9,k)} + C_{23}^{(9,k)}) + (t, b, C^{(7)}, C^{(9)} \rightarrow b, t, C^{(8)}, C^{(10)})\},
\end{aligned}$$

$$\begin{aligned}
g_{14}(k_1, k_2) &= \frac{-ie}{32\pi^2} \sum_{k=1,2} \left\{ F_1^{t\bar{b}_k\bar{\chi}_1^+} \left[Q_b(C_{12}^{(7,k)} + 2C_{22}^{(7,k)}) + 2Q_t(C_{12}^{(9,k)} + C_{22}^{(9,k)}) \right] \right. \\
& + (t, b, C^{(7)}, C^{(9)} \rightarrow b, t, C^{(8)}, C^{(10)})\},
\end{aligned}$$

$$\begin{aligned}
g_{15}(k_1, k_2) &= \frac{ie}{32\pi^2} \sum_{k=1,2} \left\{ m_t F_2^{t\bar{b}_k\bar{\chi}_1^+} \left[Q_b(C_0^{(7,k)} + 2C_{11}^{(7,k)} - 2C_{12}^{(7,k)}) - 2Q_t(C_0^{(9,k)} + C_{11}^{(9,k)} \right. \right. \\
& - C_{12}^{(9,k)}) \left. \right] + (t, b, C^{(7)}, C^{(9)} \rightarrow b, t, C^{(8)}, C^{(10)})\},
\end{aligned}$$

$$\begin{aligned}
g_{16}(k_1, k_2) &= \frac{-ie}{32\pi^2} \sum_{k=1,2} \left\{ m_t F_2^{t\bar{b}_k\bar{\chi}_1^+} \left[Q_b(C_0^{(7,k)} + 2C_{12}^{(7,k)}) - 2Q_t C_{12}^{(9,k)} \right] \right. \\
& + (t, b, C^{(7)}, C^{(9)} \rightarrow b, t, C^{(8)}, C^{(10)})\},
\end{aligned}$$

$$g_{17}(k_1, k_2) = \frac{-ie}{32\pi^2} \sum_{k=1,2} \left\{ Q_t F_1^{t\bar{b}_k\bar{\chi}_1^+} (C_0^{(9,k)} + C_{11}^{(9,k)}) + (t, b, C^{(9)} \rightarrow b, t, C^{(10)})\},
\right.$$

$$g_{18}(k_1, k_2) = g_{19}(k_1, k_2) = \frac{ie}{32\pi^2} \sum_{k=1,2} \left\{ m_t Q_t F_2^{t\bar{b}_k\bar{\chi}_1^+} C_0^{(9,k)} + (t, b, C^{(9)} \rightarrow b, t, C^{(10)})\},
\right.$$

$$\begin{aligned}
g_{20}(k_1, k_2) &= \frac{ie}{32\pi^2} \sum_{k=1,2} \left\{ F_1^{t\bar{b}_k\tilde{\chi}_1^+} \left[2Q_b C_{24}^{(7,k)} - Q_t(m_t^2 C_0^{(9,k)} - k_1^2 C_{11}^{(9,k)} + (k_1^2 - k_2^2) C_{12}^{(9,k)} \right. \right. \\
&- \left. \left. k_1^2 C_{21}^{(9,k)} - (k_1 + k_2)^2 C_{22}^{(9,k)} + 2(k_1^2 + k_1 \cdot k_2) C_{23}^{(9,k)} + (2 - \epsilon) C_{24}^{(9,k)} \right] \right. \\
&\left. + (t, b, C^{(7)}, C^{(9)} \rightarrow b, t, C^{(8)}, C^{(10)}) \right\}.
\end{aligned}$$

Then we can obtain the form factors in the renormalized amplitude of the t-channel vertex diagrams in the subprocess $\gamma\gamma \rightarrow \tilde{\chi}_1^+ \tilde{\chi}_1^+$.

$$f_i^{v,\hat{t}} = 0 \quad (i = 2, 3, 6, 7, 9, 10, 12, 13, 16 \sim 22),$$

$$\begin{aligned}
f_1^{v,\hat{t}} &= 2ie(p_1 \cdot p_3) A_t \left\{ m_{\tilde{\chi}_1^+} [g_{17}(p_1, p_3 - p_1) + g_{17}(p_1 - p_3, p_2)] \right. \\
&- \left. g_{18}(p_1 - p_3, p_2) - g_{19}(p_1, p_3 - p_1) \right\},
\end{aligned}$$

$$f_4^{v,\hat{t}} = 2ie(p_1 \cdot p_3) A_t [g_{12}(p_1 - p_3, p_2) - g_{11}(p_1 - p_3, p_2)],$$

$$\begin{aligned}
f_5^{v,\hat{t}} &= -2ie A_t \left\{ ie [C^+ + C^-] + m_{\tilde{\chi}_1^+}^2 (g_{11}(p_1, p_3 - p_1) - g_{12}(p_1, p_3 - p_1)) \right. \\
&- g_{13}(p_1, p_3 - p_1) + g_{14}(p_1, p_3 - p_1) - g_{17}(p_1, p_3 - p_1) + g_{17}(p_1 - p_3, p_2)) \\
&+ (p_1 \cdot p_3)(g_{13}(p_1, p_3 - p_1) - g_{14}(p_1, p_3 - p_1) + 2g_{17}(p_1, p_3 - p_1)) \\
&+ m_{\tilde{\chi}_1^+} (g_{15}(p_1, p_3 - p_1) - g_{16}(p_1, p_3 - p_1) + g_{18}(p_1, p_3 - p_1) - g_{18}(p_1 - p_3, p_2) \\
&- \left. g_{19}(p_1, p_3 - p_1) - g_{19}(p_1 - p_3, p_2)) + g_{20}(p_1, p_3 - p_1) + g_{20}(p_1 - p_3, p_2) \right\},
\end{aligned}$$

$$\begin{aligned}
f_8^{v,\hat{t}} &= 2f_{14}^{v,\hat{t}} = 2ie A_t \left\{ m_{\tilde{\chi}_1^+} [g_{11}(p_1 - p_3, p_2) - g_{12}(p_1 - p_3, p_2) - g_{13}(p_1 - p_3, p_2) \right. \\
&+ g_{14}(p_1 - p_3, p_2) - 2g_{17}(p_1 - p_3, p_2)] + g_{15}(p_1 - p_3, p_2) - g_{16}(p_1 - p_3, p_2) \\
&+ \left. 2g_{18}(p_1 - p_3, p_2) \right\},
\end{aligned}$$

$$\begin{aligned}
f_{11}^{v,\hat{t}} &= -ieA_t \left\{ ie(C^+ + C^-) + m_{\tilde{\chi}_1^+}^2 (g_{17}(p_1, p_3 - p_1) + g_{17}(p_1 - p_3, p_2)) \right. \\
&\quad - m_{\tilde{\chi}_1^+} (g_{18}(p_1, p_3 - p_1) + g_{18}(p_1 - p_3, p_2) + g_{19}(p_1, p_3 - p_1) \\
&\quad + g_{19}(p_1 - p_3, p_2)) + g_{20}(p_1, p_3 - p_1) + g_{20}(p_1 - p_3, p_2) \left. \right\}, \\
f_{15}^{v,\hat{t}} &= f_{14}^{v,\hat{t}} (g_i(p_1 - p_3, p_2) \rightarrow g_i(p_1, p_3 - p_1)).
\end{aligned}$$

The form factors from the renormalized amplitude of t-channel box diagrams Fig.1(c) are written as:

$$\begin{aligned}
f_1^{b,\hat{t}} &= \left\{ \frac{-ie^2 Q_b^2}{32\pi^2} \sum_{k=1,2} F_1^{b\tilde{t}_k\tilde{\chi}_1^+} m_{\tilde{\chi}_1^+} \left[2p_1 \cdot p_2 (D_{13}^{(1,k)} + D_{35}^{(1,k)} + 2D_{25}^{(1,k)} - D_{23}^{(1,k)} - D_{37}^{(1,k)}) \right. \right. \\
&\quad + 2p_1 \cdot p_3 (D_{11}^{(1,k)} + D_{12}^{(1,k)} + D_{21}^{(1,k)} + D_{23}^{(1,k)} + D_{34}^{(1,k)} + D_{37}^{(1,k)} + 2D_{24}^{(1,k)} - 3D_{25}^{(1,k)} \\
&\quad - D_{26}^{(1,k)} - D_{310}^{(1,k)} - D_{35}^{(1,k)} - 2D_{13}^{(1,k)}) + 2p_2 \cdot p_3 (D_{23}^{(1,k)} + D_{37}^{(1,k)} - D_{13}^{(1,k)} - D_{25}^{(1,k)} \\
&\quad - D_{26}^{(1,k)} - D_{310}^{(1,k)}) + m_{\tilde{\chi}_1^+}^2 (2D_{13}^{(1,k)} + 2D_{35}^{(1,k)} + 4D_{25}^{(1,k)} - 3D_{11}^{(1,k)} - 3D_{21}^{(1,k)} - 2D_{23}^{(1,k)} \\
&\quad - 2D_{37}^{(1,k)} - D_0^{(1,k)} - D_{31}^{(1,k)}) + m_b^2 (D_0^{(1,k)} + D_{11}^{(1,k)}) + 4D_{27}^{(1,k)} + (4 - \epsilon)D_{311}^{(1,k)} \left. \right] \\
&\quad + F_2^{b\tilde{t}_k\tilde{\chi}_1^+} m_b \left[2p_1 \cdot p_2 (D_{13}^{(1,k)} + D_{25}^{(1,k)} - D_{23}^{(1,k)}) + 2p_1 \cdot p_3 (D_{11}^{(1,k)} + D_{12}^{(1,k)} \right. \\
&\quad + D_{23}^{(1,k)} + D_{24}^{(1,k)} - D_{25}^{(1,k)} - D_{26}^{(1,k)} - 2D_{13}^{(1,k)}) + 2p_2 \cdot p_3 (D_{23}^{(1,k)} - D_{13}^{(1,k)} - D_{26}^{(1,k)}) \\
&\quad + m_{\tilde{\chi}_1^+}^2 (2D_{13}^{(1,k)} + 2D_{25}^{(1,k)} - 2D_{11}^{(1,k)} - 2D_{23}^{(1,k)} - D_0^{(1,k)} - D_{21}^{(1,k)}) + m_b^2 D_0^{(1,k)} + 2D_{27}^{(1,k)} \left. \right] \\
&\quad + (b, t, F_{1,2}, D^{(1,k)} \rightarrow t, b, -F_{1,2}, D^{(2,k)}) \left. \right\} \\
&\quad - \left\{ \frac{ie^2 Q_t^2}{16\pi^2} \sum_{k=1,2} (F_1^{b\tilde{t}_k\tilde{\chi}_1^+} m_{\tilde{\chi}_1^+} D_{311}^{(3,k)} - F_2^{b\tilde{t}_k\tilde{\chi}_1^+} m_b D_{27}^{(3,k)}) + (b, t, F_{1,2}, D^{(3,k)} \rightarrow t, b, -F_{1,2}, D^{(4,k)}) \right\} \\
&\quad - \left\{ \frac{ie^2 Q_b Q_t}{16\pi^2} \sum_{k=1,2} F_1^{b\tilde{t}_k\tilde{\chi}_1^+} m_{\tilde{\chi}_1^+} (D_{311}^{(5,k)} - D_{313}^{(5,k)}) - F_2^{b\tilde{t}_k\tilde{\chi}_1^+} m_b D_{27}^{(5,k)} \right. \\
&\quad \left. + (b, t, F_{1,2}, D^{(5,k)} \rightarrow t, b, -F_{1,2}, D^{(6,k)}) \right\},
\end{aligned}$$

$$\begin{aligned}
f_2^{b,\hat{t}} = & \left\{ \frac{ie^2 Q_b^2}{16\pi^2} \sum_{k=1,2} F_1^{b\tilde{t}_k\tilde{\chi}_1^+} m_{\tilde{\chi}_1^+} (D_{27}^{(1,k)} + D_{311}^{(1,k)}) + F_2^{b\tilde{t}_k\tilde{\chi}_1^+} m_b D_{27}^{(1,k)} \right. \\
& \left. + (b, t, F_{1,2}, D^{(1,k)} \rightarrow t, b, -F_{1,2}, D^{(2,k)}) \right\} \\
& - \left\{ \frac{ie^2 Q_t^2}{16\pi^2} \sum_{k=1,2} (F_1^{b\tilde{t}_k\tilde{\chi}_1^+} m_{\tilde{\chi}_1^+} D_{311}^{(3,k)} - F_2^{b\tilde{t}_k\tilde{\chi}_1^+} m_b D_{27}^{(3,k)}) + (b, t, F_{1,2}, D^{(3,k)} \rightarrow t, b, -F_{1,2}, D^{(4,k)}) \right\} \\
& - \left\{ \frac{ie^2 Q_b Q_t}{16\pi^2} \sum_{k=1,2} F_1^{b\tilde{t}_k\tilde{\chi}_1^+} m_{\tilde{\chi}_1^+} (D_{311}^{(5,k)} - D_{313}^{(5,k)}) - F_2^{b\tilde{t}_k\tilde{\chi}_1^+} m_b D_{27}^{(5,k)} \right. \\
& \left. + (b, t, F_{1,2}, D^{(5,k)} \rightarrow t, b, -F_{1,2}, D^{(6,k)}) \right\},
\end{aligned}$$

$$\begin{aligned}
f_3^{b,\hat{t}} = & \left\{ \frac{-ie^2 Q_b^2}{16\pi^2} \sum_{k=1,2} F_1^{b\tilde{t}_k\tilde{\chi}_1^+} \left[2p_1 \cdot p_2 (D_{25}^{(1,k)} + D_{35}^{(1,k)} + D_{39}^{(1,k)} - D_{26}^{(1,k)} - D_{310}^{(1,k)} - D_{37}^{(1,k)}) \right. \right. \\
& + 2p_1 \cdot p_3 (D_{24}^{(1,k)} + D_{26}^{(1,k)} + D_{34}^{(1,k)} + D_{37}^{(1,k)} + D_{38}^{(1,k)} - D_{22}^{(1,k)} - D_{25}^{(1,k)} - D_{35}^{(1,k)} \\
& - D_{36}^{(1,k)} - D_{39}^{(1,k)}) + 2p_2 \cdot p_3 (D_{26}^{(1,k)} + D_{37}^{(1,k)} + D_{38}^{(1,k)} - D_{25}^{(1,k)} - D_{310}^{(1,k)} - D_{39}^{(1,k)}) \\
& + m_{\tilde{\chi}_1^+}^2 (D_{12}^{(1,k)} + D_{34}^{(1,k)} + 2D_{24}^{(1,k)} + 2D_{25}^{(1,k)} + 2D_{35}^{(1,k)} + 2D_{39}^{(1,k)} - D_{11}^{(1,k)} - D_{31}^{(1,k)} \\
& - 2D_{21}^{(1,k)} - 2D_{26}^{(1,k)} - 2D_{310}^{(1,k)} - 2D_{37}^{(1,k)}) + m_b^2 (D_{11}^{(1,k)} - D_{12}^{(1,k)}) + (4 - \epsilon)(D_{311}^{(1,k)} - D_{312}^{(1,k)}) \left. \right] \\
& \left. + (b, t, F_{1,2}, D^{(1,k)} \rightarrow t, b, -F_{1,2}, D^{(2,k)}) \right\} \\
& - \left\{ \frac{ie^2 Q_t^2}{8\pi^2} \sum_{k=1,2} F_1^{b\tilde{t}_k\tilde{\chi}_1^+} (D_{311}^{(3,k)} - D_{312}^{(3,k)}) + (b, t, F_{1,2}, D^{(3,k)} \rightarrow t, b, -F_{1,2}, D^{(4,k)}) \right\} \\
& - \left\{ \frac{ie^2 Q_b Q_t}{8\pi^2} \sum_{k=1,2} F_1^{b\tilde{t}_k\tilde{\chi}_1^+} (D_{311}^{(5,k)} - D_{312}^{(5,k)}) + (b, t, F_{1,2}, D^{(5,k)} \rightarrow t, b, -F_{1,2}, D^{(6,k)}) \right\},
\end{aligned}$$

$$\begin{aligned}
f_4^{b,\hat{t}} = & \left\{ \frac{-ie^2 Q_b^2}{16\pi^2} \sum_{k=1,2} F_1^{b\tilde{t}_k\tilde{\chi}_1^+} \left[2p_1 \cdot p_2 (D_{23}^{(1,k)} + D_{37}^{(1,k)} + D_{39}^{(1,k)} - D_{26}^{(1,k)} - D_{310}^{(1,k)} - D_{33}^{(1,k)}) \right. \right. \\
& + 2p_1 \cdot p_3 (2D_{26}^{(1,k)} + 2D_{310}^{(1,k)} + D_{25}^{(1,k)} + D_{33}^{(1,k)} + D_{38}^{(1,k)} - 2D_{23}^{(1,k)} - 2D_{39}^{(1,k)} - D_{22}^{(1,k)} \\
& - D_{36}^{(1,k)} - D_{37}^{(1,k)}) + 2p_2 \cdot p_3 (D_{26}^{(1,k)} + D_{33}^{(1,k)} + D_{38}^{(1,k)} - 2D_{39}^{(1,k)} - D_{23}^{(1,k)}) \\
& \left. \right] \\
& + (b, t, F_{1,2}, D^{(1,k)} \rightarrow t, b, -F_{1,2}, D^{(2,k)}) \right\}
\end{aligned}$$

$$\begin{aligned}
& +m_{\tilde{\chi}_1^+}^2(D_{12}^{(1,k)} + D_{34}^{(1,k)} + 2D_{23}^{(1,k)} + 2D_{24}^{(1,k)} + 2D_{37}^{(1,k)} + 2D_{39}^{(1,k)} - D_{13}^{(1,k)} - D_{35}^{(1,k)} \\
& - 2D_{25}^{(1,k)} - 2D_{26}^{(1,k)} - 2D_{310}^{(1,k)} - 2D_{33}^{(1,k)}) + m_b^2(D_{13}^{(1,k)} - D_{12}^{(1,k)}) \\
& + (6 - \epsilon)D_{313}^{(1,k)} - 2D_{27}^{(1,k)} - (4 - \epsilon)D_{312}^{(1,k)}] + (b, t, F_{1,2}, D^{(1,k)} \rightarrow t, b, -F_{1,2}, D^{(2,k)}) \Big\} \\
& + \left\{ \frac{ie^2 Q_t^2}{8\pi^2} \sum_{k=1,2} F_1^{b\tilde{t}_k\tilde{\chi}_1^+} (D_{27}^{(3,k)} + D_{312}^{(3,k)}) + (b, t, F_{1,2}, D^{(3,k)} \rightarrow t, b, -F_{1,2}, D^{(4,k)}) \right\} \\
& - \left\{ \frac{ie^2 Q_b Q_t}{8\pi^2} \sum_{k=1,2} F_1^{b\tilde{t}_k\tilde{\chi}_1^+} (D_{313}^{(5,k)} - D_{27}^{(5,k)} - D_{312}^{(5,k)}) + (b, t, F_{1,2}, D^{(5,k)} \rightarrow t, b, -F_{1,2}, D^{(6,k)}) \right\},
\end{aligned}$$

$$\begin{aligned}
f_5^{b,\hat{t}} &= \left\{ \frac{-ie^2 Q_b^2}{16\pi^2} \sum_{k=1,2} F_1^{b\tilde{t}_k\tilde{\chi}_1^+} \left[2p_2 \cdot p_3 (D_{25}^{(1,k)} - D_{26}^{(1,k)}) + m_{\tilde{\chi}_1^+}^2 (D_0^{(1,k)} + D_{21}^{(1,k)} + 2D_{11}^{(1,k)} \right. \right. \\
& \left. \left. - 2D_{13}^{(1,k)} - 2D_{25}^{(1,k)}) + m_b^2 D_0^{(1,k)} + 2(D_{313}^{(1,k)} - D_{311}^{(1,k)}) \right] + 2F_2^{b\tilde{t}_k\tilde{\chi}_1^+} m_b m_{\tilde{\chi}_1^+} \cdot \right. \\
& \left. (D_0^{(1,k)} + D_{11}^{(1,k)} - D_{13}^{(1,k)}) + (b, t, F_{1,2}, D^{(1,k)} \rightarrow t, b, -F_{1,2}, D^{(2,k)}) \right\} \\
& - \left\{ \frac{ie^2 Q_t^2}{8\pi^2} \sum_{k=1,2} F_1^{b\tilde{t}_k\tilde{\chi}_1^+} (D_{27}^{(3,k)} + D_{311}^{(3,k)} - D_{313}^{(3,k)}) + (b, t, F_{1,2}, D^{(3,k)} \rightarrow t, b, -F_{1,2}, D^{(4,k)}) \right\} \\
& - \left\{ \frac{ie^2 Q_b Q_t}{16\pi^2} \sum_{k=1,2} F_1^{b\tilde{t}_k\tilde{\chi}_1^+} \left[2p_1 \cdot p_2 (2D_{25}^{(5,k)} + D_{13}^{(5,k)} + D_{35}^{(5,k)}) - 2p_1 \cdot p_3 (2D_{24}^{(5,k)} + D_{12}^{(5,k)} \right. \right. \\
& \left. \left. + D_{34}^{(5,k)}) - 2p_2 \cdot p_3 (D_{13}^{(5,k)} + D_{25}^{(5,k)} + D_{26}^{(5,k)} + D_{310}^{(5,k)}) - m_b^2 (D_0^{(5,k)} + D_{11}^{(5,k)}) \right. \right. \\
& \left. \left. + m_{\tilde{\chi}_1^+}^2 (3D_{21}^{(5,k)} + D_{23}^{(5,k)} + D_{31}^{(5,k)} + D_{37}^{(5,k)} + 2D_{11}^{(5,k)}) - 4D_{27}^{(5,k)} - (4 - \epsilon)D_{311}^{(5,k)} \right] \right. \\
& \left. - F_2^{b\tilde{t}_k\tilde{\chi}_1^+} 2m_b m_{\tilde{\chi}_1^+} (D_0^{(5,k)} + D_{11}^{(5,k)}) + (b, t, F_{1,2}, D^{(5,k)} \rightarrow t, b, -F_{1,2}, D^{(6,k)}) \right\},
\end{aligned}$$

$$\begin{aligned}
f_6^{b,\hat{t}} &= \left\{ \frac{-ie^2 Q_b^2}{16\pi^2} \sum_{k=1,2} F_1^{b\tilde{t}_k\tilde{\chi}_1^+} \left[2p_1 \cdot p_2 (D_{33}^{(1,k)} - D_{37}^{(1,k)}) + 2p_1 \cdot p_3 (D_{23}^{(1,k)} + D_{37}^{(1,k)} + D_{39}^{(1,k)} \right. \right. \\
& \left. \left. - D_{25}^{(1,k)} - D_{310}^{(1,k)} - D_{33}^{(1,k)}) + 2p_2 \cdot p_3 (D_{39}^{(1,k)} - D_{33}^{(1,k)}) + m_{\tilde{\chi}_1^+}^2 (D_{35}^{(1,k)} + 2D_{33}^{(1,k)} \right. \right. \\
& \left. \left. - D_{13}^{(1,k)} - 2D_{37}^{(1,k)}) - m_b^2 D_{13}^{(1,k)} - (4 - \epsilon)D_{313}^{(1,k)} \right] - 2F_2^{b\tilde{t}_k\tilde{\chi}_1^+} m_b m_{\tilde{\chi}_1^+} D_{13}^{(1,k)} \right\}
\end{aligned}$$

$$\begin{aligned}
& + (b, t, F_{1,2}, D^{(1,k)} \rightarrow t, b, -F_{1,2}, D^{(2,k)}) \Big\} \\
& + \left\{ \frac{ie^2 Q_t^2}{8\pi^2} \sum_{k=1,2} F_1^{b\tilde{t}_k \tilde{\chi}_1^+} D_{313}^{(3,k)} + (b, t, F_{1,2}, D^{(3,k)} \rightarrow t, b, -F_{1,2}, D^{(4,k)}) \right\} \\
& - \left\{ \frac{ie^2 Q_b Q_t}{16\pi^2} \sum_{k=1,2} F_1^{b\tilde{t}_k \tilde{\chi}_1^+} \left[2p_1 \cdot p_2 (D_{23}^{(5,k)} + D_{37}^{(5,k)}) - 2p_1 \cdot p_3 (D_{26}^{(5,k)} + D_{310}^{(5,k)}) \right. \right. \\
& \quad - 2p_2 \cdot p_3 (D_{23}^{(5,k)} + D_{39}^{(5,k)}) - m_b^2 D_{13}^{(5,k)} + m_{\tilde{\chi}_1^+}^2 (D_{33}^{(5,k)} + D_{35}^{(5,k)} + 2D_{25}^{(5,k)}) \\
& \quad \left. \left. - (4 - \epsilon) D_{313}^{(5,k)} \right] - 2F_2^{b\tilde{t}_k \tilde{\chi}_1^+} m_b m_{\tilde{\chi}_1^+} D_{13}^{(5,k)} + (b, t, F_{1,2}, D^{(5,k)} \rightarrow t, b, -F_{1,2}, D^{(6,k)}) \right\}, \\
f_7^{b,\hat{t}} &= \left\{ \frac{-ie^2 Q_b^2}{8\pi^2} \sum_{k=1,2} F_1^{b\tilde{t}_k \tilde{\chi}_1^+} m_{\tilde{\chi}_1^+} (D_{11}^{(1,k)} - D_{12}^{(1,k)} + 2D_{21}^{(1,k)} - 2D_{24}^{(1,k)} - D_{25}^{(1,k)} + D_{26}^{(1,k)} \right. \\
& \quad + D_{31}^{(1,k)} + D_{310}^{(1,k)} - D_{34}^{(1,k)} - D_{35}^{(1,k)}) + F_2^{b\tilde{t}_k \tilde{\chi}_1^+} m_b (D_{11}^{(1,k)} - D_{12}^{(1,k)} + D_{21}^{(1,k)} \\
& \quad - D_{24}^{(1,k)} - D_{25}^{(1,k)} + D_{26}^{(1,k)}) + (b, t, F_{1,2}, D^{(1,k)} \rightarrow t, b, -F_{1,2}, D^{(2,k)}) \Big\} \\
& - \left\{ \frac{ie^2 Q_t^2}{8\pi^2} \sum_{k=1,2} F_1^{b\tilde{t}_k \tilde{\chi}_1^+} m_{\tilde{\chi}_1^+} (D_{24}^{(3,k)} + D_{34}^{(3,k)} + D_{35}^{(3,k)} - D_{21}^{(3,k)} - D_{310}^{(3,k)} - D_{31}^{(3,k)}) \right. \\
& \quad + F_2^{b\tilde{t}_k \tilde{\chi}_1^+} m_b (D_{11}^{(3,k)} + D_{21}^{(3,k)} + D_{26}^{(3,k)} - D_{12}^{(3,k)} - D_{24}^{(3,k)} - D_{25}^{(3,k)}) \\
& \quad + (b, t, F_{1,2}, D^{(3,k)} \rightarrow t, b, -F_{1,2}, D^{(4,k)}) \Big\} \\
& - \left\{ \frac{ie^2 Q_b Q_t}{8\pi^2} \sum_{k=1,2} F_1^{b\tilde{t}_k \tilde{\chi}_1^+} m_{\tilde{\chi}_1^+} (D_{24}^{(5,k)} + D_{25}^{(5,k)} + D_{34}^{(5,k)} + D_{35}^{(5,k)} - D_{21}^{(5,k)} - D_{26}^{(5,k)} \right. \\
& \quad - D_{310}^{(5,k)} - D_{31}^{(5,k)}) + F_2^{b\tilde{t}_k \tilde{\chi}_1^+} m_b (D_{11}^{(5,k)} + D_{21}^{(5,k)} - D_{12}^{(5,k)} - D_{24}^{(5,k)}) \\
& \quad \left. + (b, t, F_{1,2}, D^{(5,k)} \rightarrow t, b, -F_{1,2}, D^{(6,k)}) \right\}, \\
f_8^{b,\hat{t}} &= \left\{ \frac{-ie^2 Q_b^2}{8\pi^2} \sum_{k=1,2} F_1^{b\tilde{t}_k \tilde{\chi}_1^+} m_{\tilde{\chi}_1^+} (D_{26}^{(1,k)} + D_{310}^{(1,k)} - 2D_{24}^{(1,k)} - D_{12}^{(1,k)} - D_{34}^{(1,k)}) \right. \\
& \quad + F_2^{b\tilde{t}_k \tilde{\chi}_1^+} m_b (D_{26}^{(1,k)} - D_{12}^{(1,k)} - D_{24}^{(1,k)}) \\
& \quad \left. + (b, t, F_{1,2}, D^{(1,k)} \rightarrow t, b, -F_{1,2}, D^{(2,k)}) \right\}
\end{aligned}$$

$$\begin{aligned}
& - \left\{ \frac{ie^2 Q_t^2}{8\pi^2} \sum_{k=1,2} F_1^{b\tilde{t}_k\tilde{\chi}_1^+} m_{\tilde{\chi}_1^+} (D_{11}^{(3,k)} + D_{21}^{(3,k)} + D_{24}^{(3,k)} + D_{34}^{(3,k)} - D_{25}^{(3,k)} - D_{310}^{(3,k)}) \right. \\
& \quad + F_2^{b\tilde{t}_k\tilde{\chi}_1^+} m_b (-D_0^{(3,k)} + D_{13}^{(3,k)} + D_{26}^{(3,k)} - D_{11}^{(3,k)} - D_{12}^{(3,k)} - D_{24}^{(3,k)}) \\
& \quad \left. + (b, t, F_{1,2}, D^{(3,k)} \rightarrow t, b, -F_{1,2}, D^{(4,k)}) \right\} \\
& - \left\{ \frac{ie^2 Q_b Q_t}{8\pi^2} \sum_{k=1,2} F_1^{b\tilde{t}_k\tilde{\chi}_1^+} m_{\tilde{\chi}_1^+} (D_{11}^{(5,k)} + D_{21}^{(5,k)} + D_{23}^{(5,k)} + D_{24}^{(5,k)} + D_{34}^{(5,k)} + D_{37}^{(5,k)} \right. \\
& \quad - 2D_{25}^{(5,k)} - D_{13}^{(5,k)} - D_{26}^{(5,k)} - D_{310}^{(5,k)} - D_{35}^{(5,k)}) + F_2^{b\tilde{t}_k\tilde{\chi}_1^+} m_b (D_{13}^{(5,k)} + D_{25}^{(5,k)} \\
& \quad \left. - D_0^{(5,k)} - D_{11}^{(5,k)} - D_{12}^{(5,k)} - D_{24}^{(5,k)}) + (b, t, F_{1,2}, D^{(5,k)} \rightarrow t, b, -F_{1,2}, D^{(6,k)}) \right\},
\end{aligned}$$

$$\begin{aligned}
f_9^{b,\hat{t}} &= \left\{ \frac{-ie^2 Q_b^2}{8\pi^2} \sum_{k=1,2} F_1^{b\tilde{t}_k\tilde{\chi}_1^+} m_{\tilde{\chi}_1^+} (D_{26}^{(1,k)} + D_{310}^{(1,k)} - D_{25}^{(1,k)} - D_{35}^{(1,k)}) \right. \\
& \quad \left. + F_2^{b\tilde{t}_k\tilde{\chi}_1^+} m_b (D_{26}^{(1,k)} - D_{25}^{(1,k)}) + (b, t, F_{1,2}, D^{(1,k)} \rightarrow t, b, -F_{1,2}, D^{(2,k)}) \right\} \\
& - \left\{ \frac{ie^2 Q_t^2}{8\pi^2} \sum_{k=1,2} F_1^{b\tilde{t}_k\tilde{\chi}_1^+} m_{\tilde{\chi}_1^+} (D_{35}^{(3,k)} - D_{310}^{(3,k)}) + F_2^{b\tilde{t}_k\tilde{\chi}_1^+} m_b (D_{26}^{(3,k)} - D_{25}^{(3,k)}) \right. \\
& \quad \left. + (b, t, F_{1,2}, D^{(3,k)} \rightarrow t, b, -F_{1,2}, D^{(4,k)}) \right\} \\
& - \left\{ \frac{ie^2 Q_b Q_t}{8\pi^2} \sum_{k=1,2} F_1^{b\tilde{t}_k\tilde{\chi}_1^+} m_{\tilde{\chi}_1^+} (D_{310}^{(5,k)} + D_{37}^{(5,k)} - D_{35}^{(5,k)} - D_{39}^{(5,k)}) \right. \\
& \quad \left. + F_2^{b\tilde{t}_k\tilde{\chi}_1^+} m_b (D_{25}^{(5,k)} - D_{26}^{(5,k)}) + (b, t, F_{1,2}, D^{(5,k)} \rightarrow t, b, -F_{1,2}, D^{(6,k)}) \right\},
\end{aligned}$$

$$\begin{aligned}
f_{10}^{b,\hat{t}} &= \left\{ \frac{-ie^2 Q_b^2}{8\pi^2} \sum_{k=1,2} F_1^{b\tilde{t}_k\tilde{\chi}_1^+} m_{\tilde{\chi}_1^+} (D_{26}^{(1,k)} + D_{310}^{(1,k)}) + F_2^{b\tilde{t}_k\tilde{\chi}_1^+} m_b D_{26}^{(1,k)} \right. \\
& \quad \left. + (b, t, F_{1,2}, D^{(1,k)} \rightarrow t, b, -F_{1,2}, D^{(2,k)}) \right\} \\
& - \left\{ \frac{ie^2 Q_t^2}{8\pi^2} \sum_{k=1,2} \left[-F_1^{b\tilde{t}_k\tilde{\chi}_1^+} m_{\tilde{\chi}_1^+} (D_{25}^{(3,k)} + D_{310}^{(3,k)}) + F_2^{b\tilde{t}_k\tilde{\chi}_1^+} m_b (D_{13}^{(3,k)} + D_{26}^{(3,k)}) \right] \right. \\
& \quad \left. + (b, t, F_{1,2}, D^{(3,k)} \rightarrow t, b, -F_{1,2}, D^{(4,k)}) \right\}
\end{aligned}$$

$$\begin{aligned}
& - \left\{ \frac{ie^2 Q_b Q_t}{8\pi^2} \sum_{k=1,2} F_1^{b\tilde{t}_k\tilde{\chi}_1^+} m_{\tilde{\chi}_1^+} (D_{25}^{(5,k)} + D_{310}^{(5,k)} + D_{33}^{(5,k)} - D_{23}^{(5,k)} - D_{37}^{(5,k)} - D_{39}^{(5,k)}) \right. \\
& \quad \left. + F_2^{b\tilde{t}_k\tilde{\chi}_1^+} m_b (D_{23}^{(5,k)} - D_{13}^{(5,k)} - D_{26}^{(5,k)}) + (b, t, F_{1,2}, D^{(5,k)} \rightarrow t, b, -F_{1,2}, D^{(6,k)}) \right\}, \\
f_{11}^{b,\hat{t}} &= \left\{ \frac{-ie^2 Q_b^2}{32\pi^2} \sum_{k=1,2} F_1^{b\tilde{t}_k\tilde{\chi}_1^+} \left[2p_1 \cdot p_2 (D_{25}^{(1,k)} - D_{26}^{(1,k)} - D_{310}^{(1,k)} - D_{33}^{(1,k)} + D_{37}^{(1,k)} + D_{39}^{(1,k)}) \right. \right. \\
& \quad + 2p_1 \cdot p_3 (-D_{22}^{(1,k)} - D_{23}^{(1,k)} + 2D_{26}^{(1,k)} + 2D_{310}^{(1,k)} + D_{33}^{(1,k)} - D_{36}^{(1,k)} - D_{37}^{(1,k)} + D_{38}^{(1,k)} \\
& \quad - 2D_{39}^{(1,k)}) + 2p_2 \cdot p_3 (D_{33}^{(1,k)} + D_{38}^{(1,k)} - 2D_{39}^{(1,k)}) + m_{\tilde{\chi}_1^+}^2 (D_0^{(1,k)} + D_{12}^{(1,k)} - D_{13}^{(1,k)} \\
& \quad - D_{21}^{(1,k)} + 2D_{24}^{(1,k)} - 2D_{26}^{(1,k)} - 2D_{310}^{(1,k)} - 2D_{33}^{(1,k)} + D_{34}^{(1,k)} - D_{35}^{(1,k)} + 2D_{37}^{(1,k)} + 2D_{39}^{(1,k)}) \\
& \quad \left. + m_b^2 (D_0^{(1,k)} - D_{12}^{(1,k)} + D_{13}^{(1,k)}) + (4 - \epsilon)(D_{313}^{(1,k)} - D_{312}^{(1,k)}) \right] + 2F_2^{b\tilde{t}_k\tilde{\chi}_1^+} m_b m_{\tilde{\chi}_1^+} D_0^{(1,k)} \\
& \quad \left. + (b, t, F_{1,2}, D^{(1,k)} \rightarrow t, b, -F_{1,2}, D^{(2,k)}) \right\} \\
& - \left\{ \frac{ie^2 Q_t^2}{16\pi^2} \sum_{k=1,2} F_1^{b\tilde{t}_k\tilde{\chi}_1^+} (D_{313}^{(3,k)} - D_{312}^{(3,k)}) + (b, t, F_{1,2}, D^{(3,k)} \rightarrow t, b, -F_{1,2}, D^{(4,k)}) \right\} \\
& + \left\{ \frac{ie^2 Q_b Q_t}{16\pi^2} \sum_{k=1,2} F_1^{b\tilde{t}_k\tilde{\chi}_1^+} (D_{27}^{(5,k)} + D_{312}^{(5,k)}) + (b, t, F_{1,2}, D^{(5,k)} \rightarrow t, b, -F_{1,2}, D^{(6,k)}) \right\}, \\
f_{12}^{b,\hat{t}} &= \left\{ \frac{-ie^2 Q_b^2}{16\pi^2} \sum_{k=1,2} F_1^{b\tilde{t}_k\tilde{\chi}_1^+} (D_{27}^{(1,k)} + D_{312}^{(1,k)} - D_{313}^{(1,k)}) + (b, t, F_{1,2}, D^{(1,k)} \rightarrow t, b, -F_{1,2}, D^{(2,k)}) \right\} \\
& - \left\{ \frac{ie^2 Q_t^2}{16\pi^2} \sum_{k=1,2} F_1^{b\tilde{t}_k\tilde{\chi}_1^+} (D_{313}^{(3,k)} - D_{312}^{(3,k)}) + (b, t, F_{1,2}, D^{(3,k)} \rightarrow t, b, -F_{1,2}, D^{(4,k)}) \right\} \\
& + \left\{ \frac{ie^2 Q_b Q_t}{16\pi^2} \sum_{k=1,2} F_1^{b\tilde{t}_k\tilde{\chi}_1^+} D_{312}^{(5,k)} + (b, t, F_{1,2}, D^{(5,k)} \rightarrow t, b, -F_{1,2}, D^{(6,k)}) \right\}, \\
f_{13}^{b,\hat{t}} &= \left\{ \frac{-ie^2 Q_b^2}{16\pi^2} \sum_{k=1,2} F_1^{b\tilde{t}_k\tilde{\chi}_1^+} m_{\tilde{\chi}_1^+} (D_{11}^{(1,k)} + D_{21}^{(1,k)} - D_{12}^{(1,k)} - D_{24}^{(1,k)}) \right. \\
& \quad \left. + F_2^{b\tilde{t}_k\tilde{\chi}_1^+} m_b (D_{11}^{(1,k)} - D_{12}^{(1,k)}) + (b, t, F_{1,2}, D^{(1,k)} \rightarrow t, b, -F_{1,2}, D^{(2,k)}) \right\},
\end{aligned}$$

$$f_{14}^{b,\hat{t}} = \left\{ \frac{ie^2 Q_b^2}{16\pi^2} \sum_{k=1,2} F_1^{b\tilde{t}_k \tilde{\chi}_1^+} m_{\tilde{\chi}_1^+} (D_{12}^{(1,k)} + D_{24}^{(1,k)}) + F_2^{b\tilde{t}_k \tilde{\chi}_1^+} m_b D_{12}^{(1,k)} \right. \\ \left. + (b, t, F_{1,2}, D^{(1,k)} \rightarrow t, b, -F_{1,2}, D^{(2,k)}) \right\},$$

$$f_{15}^{b,\hat{t}} = \left\{ \frac{-ie^2 Q_b^2}{16\pi^2} \sum_{k=1,2} F_1^{b\tilde{t}_k \tilde{\chi}_1^+} m_{\tilde{\chi}_1^+} (D_{13}^{(1,k)} + D_{25}^{(1,k)} - D_{11}^{(1,k)} - D_{21}^{(1,k)}) \right. \\ \left. + F_2^{b\tilde{t}_k \tilde{\chi}_1^+} m_b (D_{13}^{(1,k)} - D_{11}^{(1,k)}) + (b, t, F_{1,2}, D^{(1,k)} \rightarrow t, b, -F_{1,2}, D^{(2,k)}) \right\} \\ - \left\{ \frac{ie^2 Q_b Q_t}{16\pi^2} \sum_{k=1,2} F_1^{b\tilde{t}_k \tilde{\chi}_1^+} m_{\tilde{\chi}_1^+} (D_{13}^{(5,k)} + D_{25}^{(5,k)} - D_{11}^{(5,k)} - D_{21}^{(5,k)}) \right. \\ \left. + F_2^{b\tilde{t}_k \tilde{\chi}_1^+} m_b (D_0^{(5,k)} + D_{11}^{(5,k)}) + (b, t, F_{1,2}, D^{(5,k)} \rightarrow t, b, -F_{1,2}, D^{(6,k)}) \right\},$$

$$f_{16}^{b,\hat{t}} = \left\{ \frac{-ie^2 Q_b^2}{16\pi^2} \sum_{k=1,2} F_1^{b\tilde{t}_k \tilde{\chi}_1^+} m_{\tilde{\chi}_1^+} (D_{13}^{(1,k)} + D_{25}^{(1,k)}) + F_2^{b\tilde{t}_k \tilde{\chi}_1^+} m_b D_{13}^{(1,k)} \right. \\ \left. + (b, t, F_{1,2}, D^{(1,k)} \rightarrow t, b, -F_{1,2}, D^{(2,k)}) \right\} \\ - \left\{ \frac{ie^2 Q_b Q_t}{16\pi^2} \sum_{k=1,2} F_1^{b\tilde{t}_k \tilde{\chi}_1^+} m_{\tilde{\chi}_1^+} (D_{23}^{(5,k)} - D_{25}^{(5,k)}) + F_2^{b\tilde{t}_k \tilde{\chi}_1^+} m_b D_{13}^{(5,k)} \right. \\ \left. + (b, t, F_{1,2}, D^{(5,k)} \rightarrow t, b, -F_{1,2}, D^{(6,k)}) \right\},$$

$$f_{17}^{b,\hat{t}} = \left\{ \frac{-ie^2 Q_b^2}{8\pi^2} \sum_{k=1,2} F_1^{b\tilde{t}_k \tilde{\chi}_1^+} (D_{22}^{(1,k)} + D_{25}^{(1,k)} + D_{35}^{(1,k)} + D_{36}^{(1,k)} + D_{39}^{(1,k)} - D_{24}^{(1,k)} - D_{26}^{(1,k)} \right. \\ \left. - D_{34}^{(1,k)} - D_{37}^{(1,k)} - D_{38}^{(1,k)}) + (b, t, F_{1,2}, D^{(1,k)} \rightarrow t, b, -F_{1,2}, D^{(2,k)}) \right\} \\ - \left\{ \frac{ie^2 Q_t^2}{8\pi^2} \sum_{k=1,2} F_1^{b\tilde{t}_k \tilde{\chi}_1^+} (D_{24}^{(3,k)} + D_{26}^{(3,k)} + D_{34}^{(3,k)} + D_{37}^{(3,k)} + D_{38}^{(3,k)} - D_{22}^{(3,k)} - D_{25}^{(3,k)} \right. \\ \left. - D_{35}^{(3,k)} - D_{36}^{(3,k)} - D_{39}^{(3,k)}) + (b, t, F_{1,2}, D^{(3,k)} \rightarrow t, b, -F_{1,2}, D^{(4,k)}) \right\} \\ - \left\{ \frac{ie^2 Q_b Q_t}{8\pi^2} \sum_{k=1,2} F_1^{b\tilde{t}_k \tilde{\chi}_1^+} (D_{24}^{(5,k)} + D_{34}^{(5,k)} - D_{22}^{(5,k)} - D_{36}^{(5,k)}) \right. \\ \left. + (b, t, F_{1,2}, D^{(5,k)} \rightarrow t, b, -F_{1,2}, D^{(6,k)}) \right\},$$

$$\begin{aligned}
f_{18}^{b,\hat{t}} = & \left\{ \frac{-ie^2 Q_b^2}{8\pi^2} \sum_{k=1,2} F_1^{b\tilde{t}_k\tilde{\chi}_1^+} (D_{22}^{(1,k)} + D_{23}^{(1,k)} + D_{36}^{(1,k)} + D_{39}^{(1,k)} - D_{25}^{(1,k)} - D_{26}^{(1,k)} - D_{310}^{(1,k)} - D_{38}^{(1,k)}) \right. \\
& \left. + (b, t, F_{1,2}, D^{(1,k)} \rightarrow t, b, -F_{1,2}, D^{(2,k)}) \right\} \\
& - \left\{ \frac{ie^2 Q_t^2}{8\pi^2} \sum_{k=1,2} F_1^{b\tilde{t}_k\tilde{\chi}_1^+} (2D_{26}^{(3,k)} + D_{13}^{(3,k)} + D_{25}^{(3,k)} + D_{310}^{(3,k)} + D_{38}^{(3,k)} - D_{12}^{(3,k)} - D_{22}^{(3,k)} \right. \\
& \left. - D_{23}^{(3,k)} - D_{24}^{(3,k)} - D_{36}^{(3,k)} - D_{39}^{(3,k)}) + (b, t, F_{1,2}, D^{(3,k)} \rightarrow t, b, -F_{1,2}, D^{(4,k)}) \right\} \\
& - \left\{ \frac{ie^2 Q_b Q_t}{8\pi^2} \sum_{k=1,2} F_1^{b\tilde{t}_k\tilde{\chi}_1^+} (D_{13}^{(5,k)} + D_{25}^{(5,k)} + D_{26}^{(5,k)} + D_{310}^{(5,k)} - D_{12}^{(5,k)} - D_{22}^{(5,k)} - D_{24}^{(5,k)} - D_{36}^{(5,k)}) \right. \\
& \left. + (b, t, F_{1,2}, D^{(5,k)} \rightarrow t, b, -F_{1,2}, D^{(6,k)}) \right\},
\end{aligned}$$

$$\begin{aligned}
f_{19}^{b,\hat{t}} = & \left\{ \frac{-ie^2 Q_b^2}{8\pi^2} \sum_{k=1,2} F_1^{b\tilde{t}_k\tilde{\chi}_1^+} (D_{25}^{(1,k)} + D_{310}^{(1,k)} + D_{39}^{(1,k)} - D_{26}^{(1,k)} - D_{37}^{(1,k)} - D_{38}^{(1,k)}) \right. \\
& \left. + (b, t, F_{1,2}, D^{(1,k)} \rightarrow t, b, -F_{1,2}, D^{(2,k)}) \right\} \\
& - \left\{ \frac{ie^2 Q_t^2}{8\pi^2} \sum_{k=1,2} F_1^{b\tilde{t}_k\tilde{\chi}_1^+} (D_{37}^{(3,k)} + D_{38}^{(3,k)} - D_{310}^{(3,k)} - D_{39}^{(3,k)}) \right. \\
& \left. + (b, t, F_{1,2}, D^{(3,k)} \rightarrow t, b, -F_{1,2}, D^{(4,k)}) \right\} \\
& - \left\{ \frac{ie^2 Q_b Q_t}{8\pi^2} \sum_{k=1,2} F_1^{b\tilde{t}_k\tilde{\chi}_1^+} (D_{310}^{(5,k)} - D_{38}^{(5,k)}) + (b, t, F_{1,2}, D^{(5,k)} \rightarrow t, b, -F_{1,2}, D^{(6,k)}) \right\},
\end{aligned}$$

$$\begin{aligned}
f_{20}^{b,\hat{t}} = & \left\{ \frac{-ie^2 Q_b^2}{8\pi^2} \sum_{k=1,2} F_1^{b\tilde{t}_k\tilde{\chi}_1^+} (D_{23}^{(1,k)} + D_{39}^{(1,k)} - D_{26}^{(1,k)} - D_{38}^{(1,k)}) \right. \\
& \left. + (b, t, F_{1,2}, D^{(1,k)} \rightarrow t, b, -F_{1,2}, D^{(2,k)}) \right\} \\
& - \left\{ \frac{ie^2 Q_t^2}{8\pi^2} \sum_{k=1,2} F_1^{b\tilde{t}_k\tilde{\chi}_1^+} (D_{26}^{(3,k)} + D_{38}^{(3,k)} - D_{23}^{(3,k)} - D_{39}^{(3,k)}) \right. \\
& \left. + (b, t, F_{1,2}, D^{(3,k)} \rightarrow t, b, -F_{1,2}, D^{(4,k)}) \right\} \\
& - \left\{ \frac{ie^2 Q_b Q_t}{8\pi^2} \sum_{k=1,2} F_1^{b\tilde{t}_k\tilde{\chi}_1^+} (D_{23}^{(5,k)} + D_{39}^{(5,k)} - D_{26}^{(5,k)} - D_{38}^{(5,k)}) \right.
\end{aligned}$$

$$+(b, t, F_{1,2}, D^{(5,k)} \rightarrow t, b, -F_{1,2}, D^{(6,k)})\},$$

$$f_i^{v,\hat{t}} = 0 \quad (i = 21 \sim 22).$$

The form factors in the renormalized amplitude of the quartic interaction diagrams Fig.1(d) are expressed as:

$$\begin{aligned} f_1^q &= f_2^q = \left\{ \frac{ie^2 Q_t^2}{32\pi^2} \sum_{k=1,2} (m_{\tilde{\chi}_1^+} C_{11}^{(1,k)} F_1^{b\tilde{t}_k \tilde{\chi}_1^+} - m_b C_0^{(1,k)} F_2^{b\tilde{t}_k \tilde{\chi}_1^+}) \right. \\ &+ \frac{e^2 Q_t^2}{16\pi^2} \sum_{k=1,2} \bar{B}_0^{(1,k)} [(V_{h^0 \tilde{t}_k \tilde{t}_k} V_{h^0 \tilde{\chi}_1^+ \tilde{\chi}_1^+}^s) A_h + (V_{H^0 \tilde{t}_k \tilde{t}_k} V_{H^0 \tilde{\chi}_1^+ \tilde{\chi}_1^+}^s) A_H] \\ &\left. + (t, b, F_{1,2}, \bar{B}^{(1,k)}, C^{(1,k)} \rightarrow b, t, -F_{1,2}, \bar{B}^{(2,k)}, C^{(2,k)}) \right\}, \end{aligned}$$

$$f_i^q = 0, \quad (i = 3 \sim 22)$$

The form factors in the renormalized amplitude from the t-channel triangle diagrams depicted in Fig.1(e), are listed below:

$$\begin{aligned} f_1^{tr,\hat{t}} &= f_2^{tr,\hat{t}} = \left\{ \frac{-e^2 Q_t^2}{8\pi^2} \sum_{k=1,2} [\bar{C}_{24}^{(3,k)} (V_{H^0 \tilde{t}_k \tilde{t}_k} V_{H^0 \tilde{\chi}_1^+ \tilde{\chi}_1^+}^s A_H + V_{h^0 \tilde{t}_k \tilde{t}_k} V_{h^0 \tilde{\chi}_1^+ \tilde{\chi}_1^+}^s A_h) \right. \\ &+ \frac{-e^2 Q_b^2}{8\pi^2} (V_{H^0 b b} V_{H^0 \tilde{\chi}_1^+ \tilde{\chi}_1^+}^s A_H + V_{h^0 b b} V_{h^0 \tilde{\chi}_1^+ \tilde{\chi}_1^+}^s A_h) [-2p_1 \cdot p_2 m_b C_{22}^{(5)} \\ &+ (p_1 \cdot p_3 + p_2 \cdot p_3) m_b (2C_{23}^{(5)} - C_0^{(5)}) + m_b^3 C_0^{(5)} - 2m_b m_{\tilde{\chi}_1^+}^2 C_{22}^{(5)} - m_b \epsilon C_{24}^{(5)}] \\ &\left. + (t, b, \bar{C}^{(3,k)}, C^{(3,k)}, C^{(5)} \rightarrow b, t, \bar{C}^{(4,k)}, C^{(4,k)}, C^{(6)}) \right\}, \end{aligned}$$

$$\begin{aligned} f_7^{tr,\hat{t}} &= f_8^{tr,\hat{t}} = f_9^{tr,\hat{t}} = f_{10}^{tr,\hat{t}} = \\ &\left\{ \frac{-e^2 Q_t^2}{4\pi^2} \sum_{k=1,2} [(C_{23}^{(3,k)} - C_{22}^{(3,k)}) (V_{H^0 \tilde{t}_k \tilde{t}_k} V_{H^0 \tilde{\chi}_1^+ \tilde{\chi}_1^+}^s A_H + V_{h^0 \tilde{t}_k \tilde{t}_k} V_{h^0 \tilde{\chi}_1^+ \tilde{\chi}_1^+}^s A_h) \right. \end{aligned}$$

$$\begin{aligned}
& - \frac{e^2 Q_b^2}{4\pi^2} \left[m_b (V_{H^0 bb} V_{H^0 \tilde{\chi}_1^+ \tilde{\chi}_1^+}^s A_H + V_{h^0 bb} V_{h^0 \tilde{\chi}_1^+ \tilde{\chi}_1^+}^s A_h) (C_0^{(5)} + 4C_{22}^{(5)} - 4C_{23}^{(5)}) \right] \\
& + (t, b, C^{(3,k)}, C^{(5)} \rightarrow b, t, C^{(4,k)}, C^{(6)}) \Big\},
\end{aligned}$$

$$\begin{aligned}
f_{21}^{tr, \hat{t}} &= f_{22}^{tr, \hat{t}} = \left\{ \frac{-im_b e^2 Q_b^2}{4\pi^2} C_0^{(5)} \left[(V_{A^0 bb} V_{A^0 \tilde{\chi}_1^+ \tilde{\chi}_1^+}^{ps} A_A + V_{G^0 bb} V_{G^0 \tilde{\chi}_1^+ \tilde{\chi}_1^+}^{ps} A_G) + (t, b, C^{(5)} \rightarrow b, t, C^{(6)}) \right] \right\}, \\
f_i^{tr, \hat{t}} &= 0, \quad (i = 3 \sim 6, 11 \sim 20),
\end{aligned}$$

where $\bar{C}_{24}^{(3,k)} = C_{24}^{(3,k)} - \frac{\Delta}{4}$ and $\bar{C}_{24}^{(4,k)} = C_{24}^{(4,k)} - \frac{\Delta}{4}$. The form factors in renormalized amplitude of the self-energy corrections $\mathcal{M}^{s, \hat{t}}$ from Fig.1(f) including t-channel, are expressed as:

$$f_i^{s, \hat{t}} = 0, \quad (i = 2 \sim 4, 6 \sim 10, 12 \sim 22),$$

$$\begin{aligned}
f_1^{s, \hat{t}} &= \frac{-ie^2 A_t^2}{16\pi^2} p_1 \cdot p_3 \sum_{k=1,2} (-B_1^{(3,k)} m_{\tilde{\chi}_1^+} F_1^{b\tilde{t}_k \tilde{\chi}_1^+} + B_0^{(3,k)} m_b F_2^{b\tilde{t}_k \tilde{\chi}_1^+} \\
& + B_1^{(4,k)} m_{\tilde{\chi}_1^+} F_1^{t\tilde{b}_k \tilde{\chi}_1^+} - B_0^{(4,k)} m_t F_2^{t\tilde{b}_k \tilde{\chi}_1^+}) - ie^2 A_t^2 p_1 \cdot p_3 [C_S^- \\
& + C_S^+ - m_{\tilde{\chi}_1^+} (C_L + C_R)]
\end{aligned}$$

$$\begin{aligned}
f_{11}^{s, \hat{t}} &= \frac{f_5^{s, \hat{t}}}{2} = \frac{-ie^2 A_t^2}{16\pi^2} \sum_{k=1,2} \left[B_1^{(3,k)} (m_{\tilde{\chi}_1^+}^2 - p_1 \cdot p_3) F_1^{b\tilde{t}_k \tilde{\chi}_1^+} \right. \\
& - B_0^{(3,k)} m_b m_{\tilde{\chi}_1^+} F_2^{b\tilde{t}_k \tilde{\chi}_1^+} \\
& - B_1^{(4,k)} (m_{\tilde{\chi}_1^+}^2 - p_1 \cdot p_3) F_1^{t\tilde{b}_k \tilde{\chi}_1^+} + B_0^{(4,k)} m_t m_{\tilde{\chi}_1^+} F_2^{t\tilde{b}_k \tilde{\chi}_1^+} \Big] \\
& - ie^2 A_t^2 [(m_{\tilde{\chi}_1^+}^2 - p_1 \cdot p_3)(C_L + C_R) - m_{\tilde{\chi}_1^+} (C_S^- + C_S^+)]
\end{aligned}$$

In this work we adopted the definitions of two-, three-, four-point one-loop Passarino-Veltman integral functions as shown in reference[30] and all the vector and tensor integrals can be deduced in the forms of scalar integrals [31].

References

- [1] S.L. Glashow, Nucl. Phys. 22(1961)579; S. Weinberg, Phys. Rev. Lett. 1(1967)1264; A. Salam, Proc. 8th Nobel Symposium Stockholm 1968, ed. N. Svartholm(Almquist and Wiksells, Stockholm 1968) p.367; H.D. Politzer, Phys. Rep. 14(1974)129.
- [2] P.W. Higgs, Phys. Lett 12(1964)132, Phys. Rev. Lett. 13 (1964)508; Phys.Rev. 145(1966)1156; F.Englert and R.Brout, Phys. Rev. Lett. 13(1964)321; G.S. Guralnik, C.R.Hagen and T.W.B. Kibble, Phys. Rev. Lett. 13(1964)585; T.W.B. Kibble, Phys. Rev. 155(1967)1554.
- [3] F. Abe et al.(CDF collaboration), Phys. Rev. Lett. **74**, 2626(1995); S. Abachi et al., (D0 collaboration), Phys. Rev. Lett. **74**, 2632(1995).
- [4] H.E. Haber and G.L. Kane, Phys. Rep. 117(1985)75.
- [5] C.X. Chang, L. Han, W.G. Ma et al Nucl. Phys. **B515** (1998)15; W. Beenakker, M. Krammer et al Nucl. Phys. **B515**(1998)3.
- [6] R. Barate et al, (ALEPH Collaboration), Eur. Phys. J. **C2** (1998)417.
- [7] P. Abreu et al, (DELPHI Collaboration), Eur. Phys. J. **C1**, 1 (1998).
- [8] M. Acciarri et al, (L3 Collaboration), Eur. Phys. J. **C4** ((1998)207.
- [9] K. Ackerstaff et al, (OPAL Collaboration), Eur. Phys. J. **C2** (1998)213.
- [10] M.A. Diaz, S.F. King and D.A. Ross, Nucl. Phys. **B529** (1998)23.

- [11] S.Y. Choi, A. Djouadi, H. Dreiner, J. Kalinowski, and P.M. Zerwas, 'Chargino Pair Production in e^+e^- Collisions', YUMS 98-10, SNUTP 98-52, DESY 98-77, PM 98-14, IFT/9/98, hep-ph/9806279; S.Y. Choi, A. Djouadi, H.S. Song and P.M. Zerwas 'Determining SUSY parameters in Chargino Pair-Production in e^+e^- Collisions' DESY 98-175, KIAS-P98038, PM/98-39, SNUTP 98-129, hep-ph/9812236.
- [12] S. Kiyoura, M.M. Nojiri, D.M. Pierce and Y. Yamada, Phys. Rev. D58, 075002.
- [13] J. Ellis and S. Rudaz, Phys. Lett. **B128**,248(1983);
- [14] S.Dimopoulos and Sutter, Nucl. Phys. **B452**(1995)496; H.Haber, Proceedings of the 5th International Conference on Supersymmetries in Physics(SUSY'97), May 1997, ed. M. Cvetcic and P.Langacker, hep-ph/9709450.
- [15] T. Ibrahim and P. Nath, Phys. Lett.**B418**(1998)98; Phys. Rev.**D57**(1998)478; Y. Kizukuri and N. Oshimo, Proceedings of the Workshop on e^+e^- Collisions at 500 GeV: The Physics Potential, Munich-Annecy-Hamburg 1991/93, DES 92-123A+B, 93-123C, ed. P.Zerwas.
- [16] S.Y. Choi, J.S. Shim, H.S. Song and W.Y. Song, YUMS 98-12, SNUTP 98-084, Aug. 1998, hep-ph/9808227.
- [17] A.Denner, Fortsch. Phys. Vol.41, No.4 (1993).
- [18] G. Altareli and R. Ruckl, Phys. Lett. **B144**(1984)126; I. Bigi and S. Rudaz, Phys. Lett. **153**(1985)335; M. Drees and M.M. Nojiri, Nucl. Phys. **B396**(1992)449.

- [19] D.M. Copper, D.R.T. Jones and P.van Nieuwenhuizen, Nucl. Phys. **B167**(1980) 479;
W. Siegel, Phys. Lett. **B84**(1979)193.
- [20] J.F. Gunion and H.E. Haber, Nucl. Phys. **B272**(1986)1.
- [21] D.A. Ross and J.C. Taylor, Nucl. Phys. **B51** (1979)25.
- [22] Bernd A. Kniehl and A. Pilaftsis, Nucl. Phys. B474(1996)286.
- [23] Han Liang, Ma Wen-Gan and Yu Zeng-Hui,, Phys. Rev. D56(1997)265.
- [24] A. Goto and T. Kon, Europhys. Lett. 13(1990) 211; 14(1991) 75; F. Cuyppers, G.J. Oldenborgh and R. Ruckl, Nucl. Phys.**B409** (1993) 144; M. Koike, T. Nonaka and T. Kon, Phys. Lett **B357** (1995)232.
- [25] M. Acciarri et al (L3 Collaboration), Phys. Lett. **B377** (1996)289.
- [26] see for examples, J.R. Espinosa, and M Quiros, Phys. Lett **B266** (1991)389; K. Gunion and A. Turski, Phys. Rev. **D39** (1989)2701 and **D40**(1990)2333; M.Carena, M. Quiros and C.E.M. Wagner, Nucl. Phys.**B461**(1996)407.
- [27] I.F. Ginzburg, G.L. Kotkin, V.G. Serbo and V.I. Telnov, Pis'ma ZHETF 34(1981)514;
Nucl. Instr. Methods 205(1983)47.
- [28] R.Blankenbecler and S.D.Drell, Phys. Rev. Lett. 61(2324)1988; F.Halzen, C.S.Kim and M.L.Stong, Phys. Lett. B274(489)1992; M.Drees and R.M.Godbole, Phys. Lett. 67(1189)1991.

[29] V.Telnov, Nucl. Instr. Methods A294(72)1990.

[30] Bernd A. Kniehl, Phys. Rep. 240(1994)211.

[31] G. Passarino and M. Veltman, Nucl. Phys. **B160**151(1979).

Figure Captions

Fig.1 Feynman diagrams involving one-loop corrections of virtual heavy quarks and squarks to the subprocess $\gamma\gamma \rightarrow \tilde{\chi}_1^+ \tilde{\chi}_1^-$. (a) tree-level diagram. (b) $\gamma\tilde{\chi}_1\tilde{\chi}_1$ vertex corrections. (c) box diagrams. (d) quartic interaction corrections. (e) triangle diagrams. (f) self-energy diagram. (g) chargino, γ and $\gamma - Z^0$ self-energy diagrams. All the u-channel diagrams are not shown here.

Fig.2 The Feynman rules for chargino-squark-quark couplings.

Fig.3 The relative correction $\hat{\delta}$ of virtual quarks and squarks to the subprocess $\gamma\gamma \rightarrow \tilde{\chi}_1^+ \tilde{\chi}_1^-$ versus the c.m.s. energy of incoming photons $\sqrt{\hat{s}}$ with $m_{\tilde{\chi}_1^+} = 165 \text{ GeV}$, $m_{\tilde{\chi}_2^+} = 750 \text{ GeV}$, $\tilde{M} = 200 \text{ GeV}$, $\phi_\mu = \phi_{\tilde{t}} = \phi_{\tilde{b}} = 0$ and $m_A = 150 \text{ GeV}$. (a) $\tan\beta = 4$. The full-line is for Higgsino-like chargino case. The dashed-line for gaugino-like chargino case. (b) $\tan\beta = 40$. The full-line is for Higgsino-like chargino case. The dashed-line for gaugino-like chargino case.

Fig.4 The relative correction $\hat{\delta}$ of virtual quarks and squarks to the subprocess $\gamma\gamma \rightarrow \tilde{\chi}_1^+ \tilde{\chi}_1^-$ versus the $\tilde{M}(M_{\tilde{Q}} = M_{\tilde{t}} = M_{\tilde{b}} = \tilde{M})$ with $\sqrt{\hat{s}} = 400 \text{ GeV}$, $m_{\tilde{\chi}_1^+} = 165 \text{ GeV}$, $m_{\tilde{\chi}_2^+} = 750 \text{ GeV}$, $\phi_\mu = \phi_{\tilde{t}} = \phi_{\tilde{b}} = 0$, $\tilde{M} = 200 \text{ GeV}$ and $m_A = 150 \text{ GeV}$. In Higgsino-like chargino case, the

full-line is for $\tan \beta = 4$ and the dotted-line is for $\tan \beta = 40$. $m_A = 150 \text{ GeV}$. In gaugino-like chargino case, the dashed-line is for $\tan \beta = 4$ and the dash-dotted-line is for $\tan \beta = 40$.

Fig.5 The relative correction $\hat{\delta}$ of virtual quarks and squarks to the subprocess $\gamma\gamma \rightarrow \tilde{\chi}_1^+ \tilde{\chi}_1^-$ versus $m_{\tilde{\chi}_1^+}$ with $\sqrt{\hat{s}} = 400 \text{ GeV}$, $m_{\tilde{\chi}_2^+} = 750 \text{ GeV}$, $\phi_\mu = \phi_{\tilde{t}} = \phi_{\tilde{b}} = 0$, $\tilde{M} = 200 \text{ GeV}$ and $m_A = 150 \text{ GeV}$. In Higgsino-like chargino case, the full-line is for $\tan \beta = 4$ and the dotted-line is for $\tan \beta = 40$. $m_A = 150 \text{ GeV}$. In gaugino-like chargino case, the dashed-line is for $\tan \beta = 4$ and the dash-dotted-line is for $\tan \beta = 40$.

Fig.6 The relative correction $\hat{\delta}$ of virtual quarks and squarks to the Higgsino-like chargino pair production subprocess $\gamma\gamma \rightarrow \tilde{\chi}_1^+ \tilde{\chi}_1^-$ versus ϕ_{CP} 's with $\sqrt{\hat{s}} = 400 \text{ GeV}$, $m_{\tilde{\chi}_1^+} = 165 \text{ GeV}$, $m_{\tilde{\chi}_2^+} = 750 \text{ GeV}$, $\tilde{M} = 200 \text{ GeV}$ and $m_A = 150 \text{ GeV}$. The full-line is for $\tan \beta = 4$ with $\phi_{CP} = \phi_{\tilde{t}} = \phi_{\tilde{b}}$. The dashed-line is for $\tan \beta = 4$ with $\phi_{CP} = \phi_\mu$. The dotted-line is for $\tan \beta = 40$ with $\phi_{CP} = \phi_{\tilde{t}} = \phi_{\tilde{b}}$. The dash-dotted-line is for $\tan \beta = 40$ with $\phi_{CP} = \phi_\mu$.

Fig.7(a) The cross section σ of the process of the Higgsino-like lightest chargino pair production via photon-photon fusion in $e^+ e^-$ collider versus the colliding energy \sqrt{s} in electron-positron c.m.s. system with $m_{\tilde{\chi}_1^+} = 165 \text{ GeV}$, $m_{\tilde{\chi}_2^+} = 750 \text{ GeV}$, $\tilde{M} = 200 \text{ GeV}$, $\phi_\mu = \phi_{\tilde{t}} = \phi_{\tilde{b}} = 0$ and $m_A = 150 \text{ GeV}$. The full-line is for $\tan \beta = 4$. The dotted-line is for $\tan \beta = 40$.

Fig.7(b) The relative correction of the process $e^+ e^- \rightarrow \gamma\gamma \rightarrow \tilde{\chi}_1^+ \tilde{\chi}_1^-$ versus the colliding energy \sqrt{s} in electron-positron c.m.s. system with $m_{\tilde{\chi}_1^+} = 165 \text{ GeV}$, $m_{\tilde{\chi}_2^+} = 750 \text{ GeV}$, $\tilde{M} = 200 \text{ GeV}$, $\phi_\mu = \phi_{\tilde{t}} = \phi_{\tilde{b}} = 0$ and $m_A = 150 \text{ GeV}$. In Higgsino-like chargino case, the full-line is for $\tan \beta = 4$ and the dotted-line is for $\tan \beta = 40$. $m_A = 150 \text{ GeV}$. In

gaugino-like chargino case, the dash-dotted-line is for $\tan \beta = 4$ and the dash-dotted-line is for $\tan \beta = 40$.

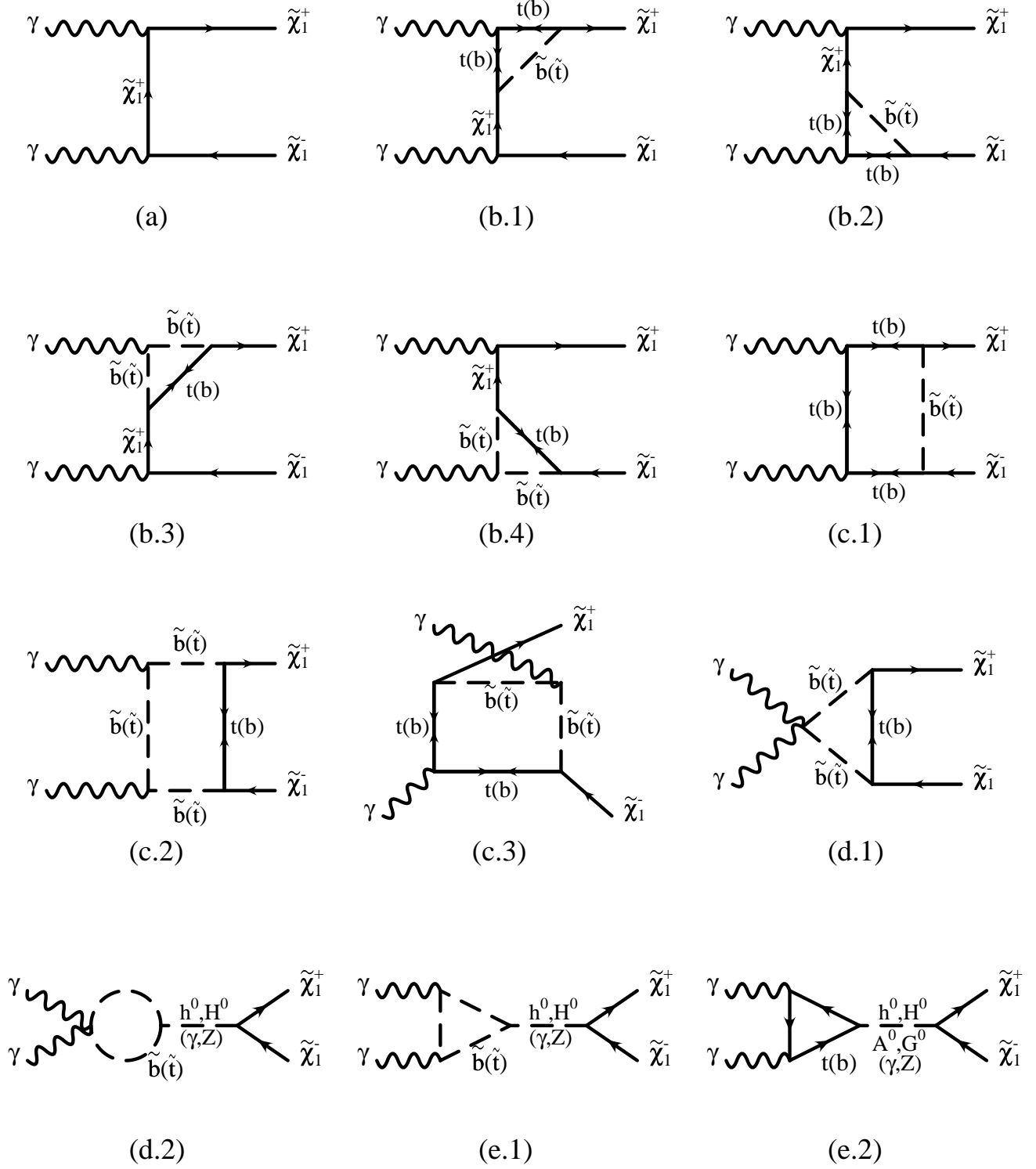


Fig.1

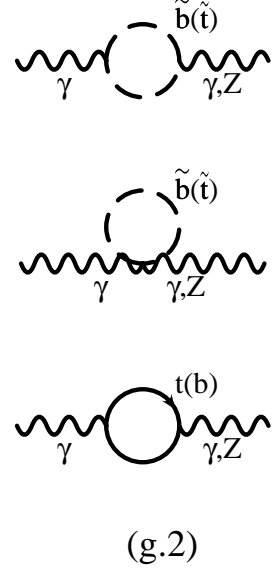
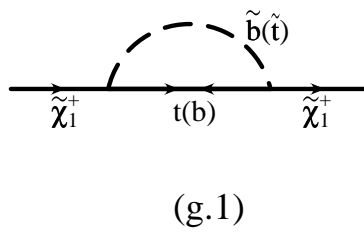
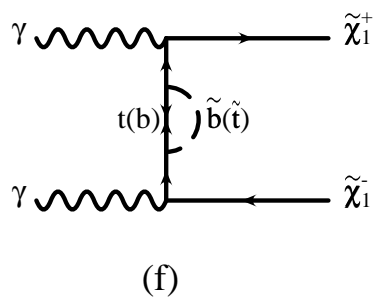
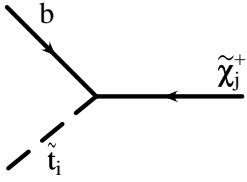
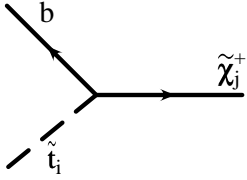


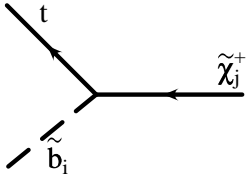
Fig.1 (continued)



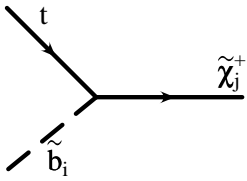
$$C^{-1}(V_{bt_i\tilde{\chi}_j}^{(1)} P_L + V_{bt_i\tilde{\chi}_j}^{(2)} P_R)$$



$$(V_{bt_i\tilde{\chi}_j}^{(2)*} P_L + V_{bt_i\tilde{\chi}_j}^{(1)*} P_R)C$$



$$(V_{tb_i\tilde{\chi}_j}^{(1)} P_L + V_{tb_i\tilde{\chi}_j}^{(2)} P_R)$$



$$(-V_{tb_i\tilde{\chi}_j}^{(2)*} P_L - V_{tb_i\tilde{\chi}_j}^{(1)*} P_R)$$

Fig.3(a)

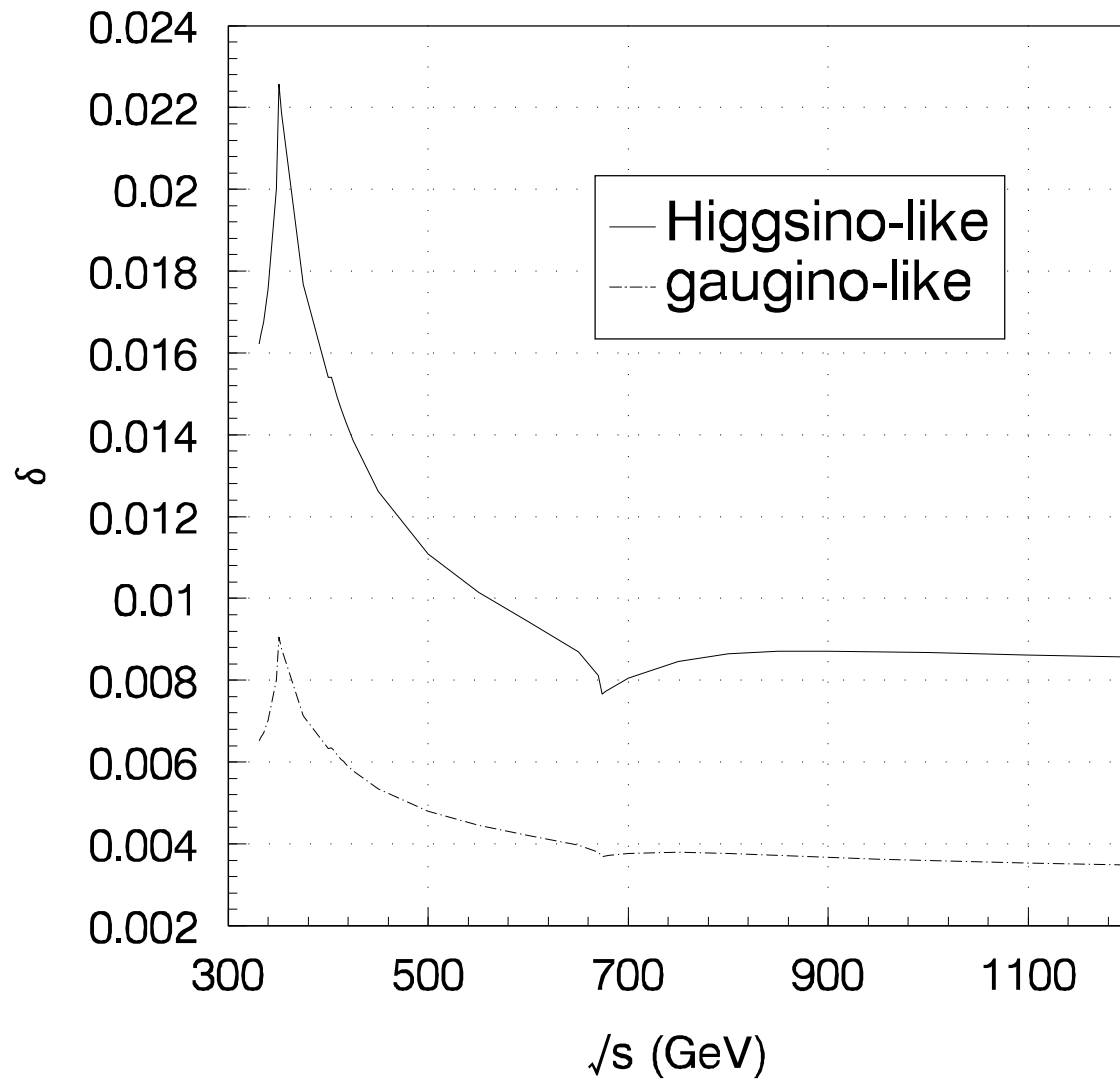


Fig.3(b)

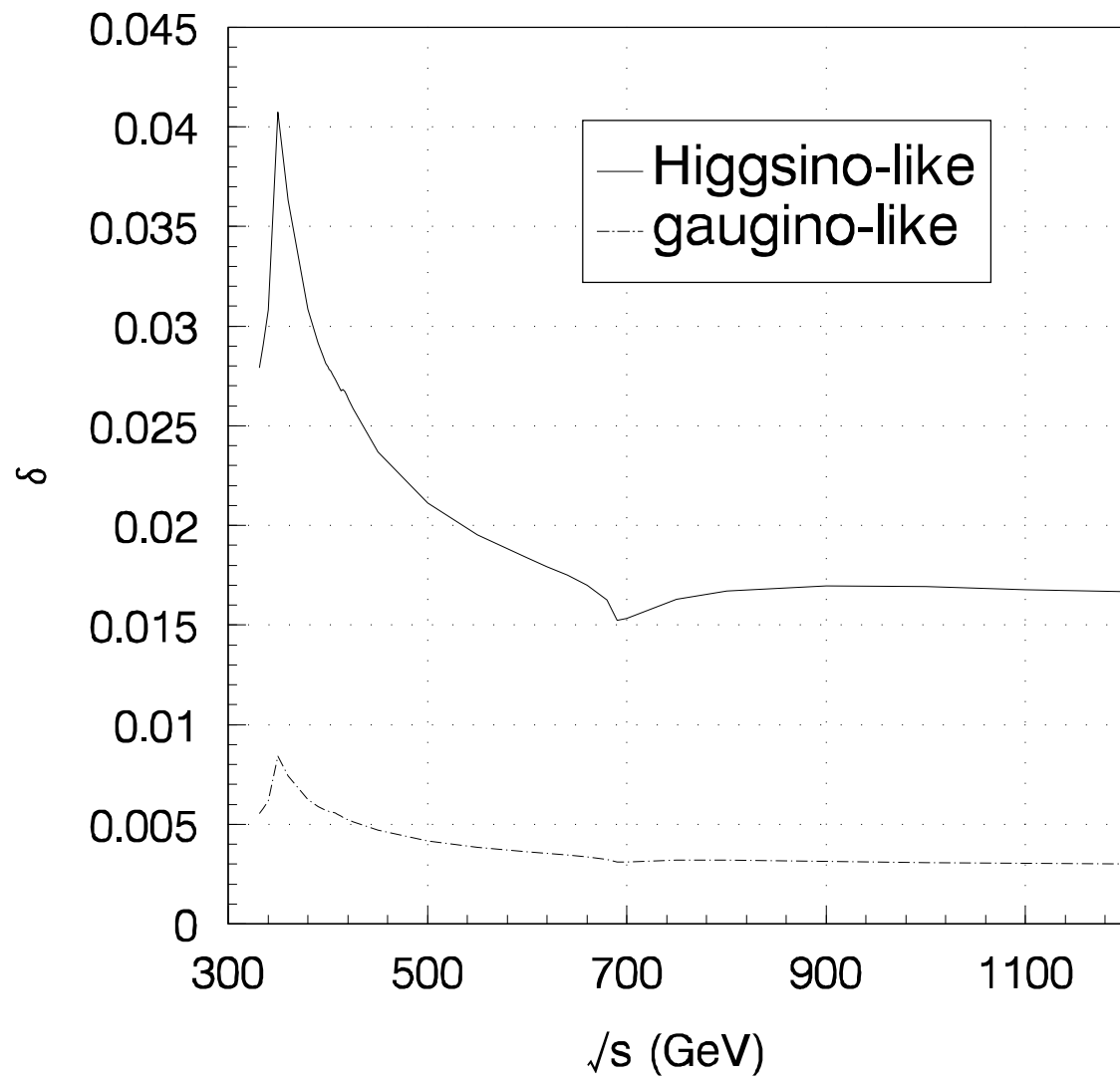


Fig.4

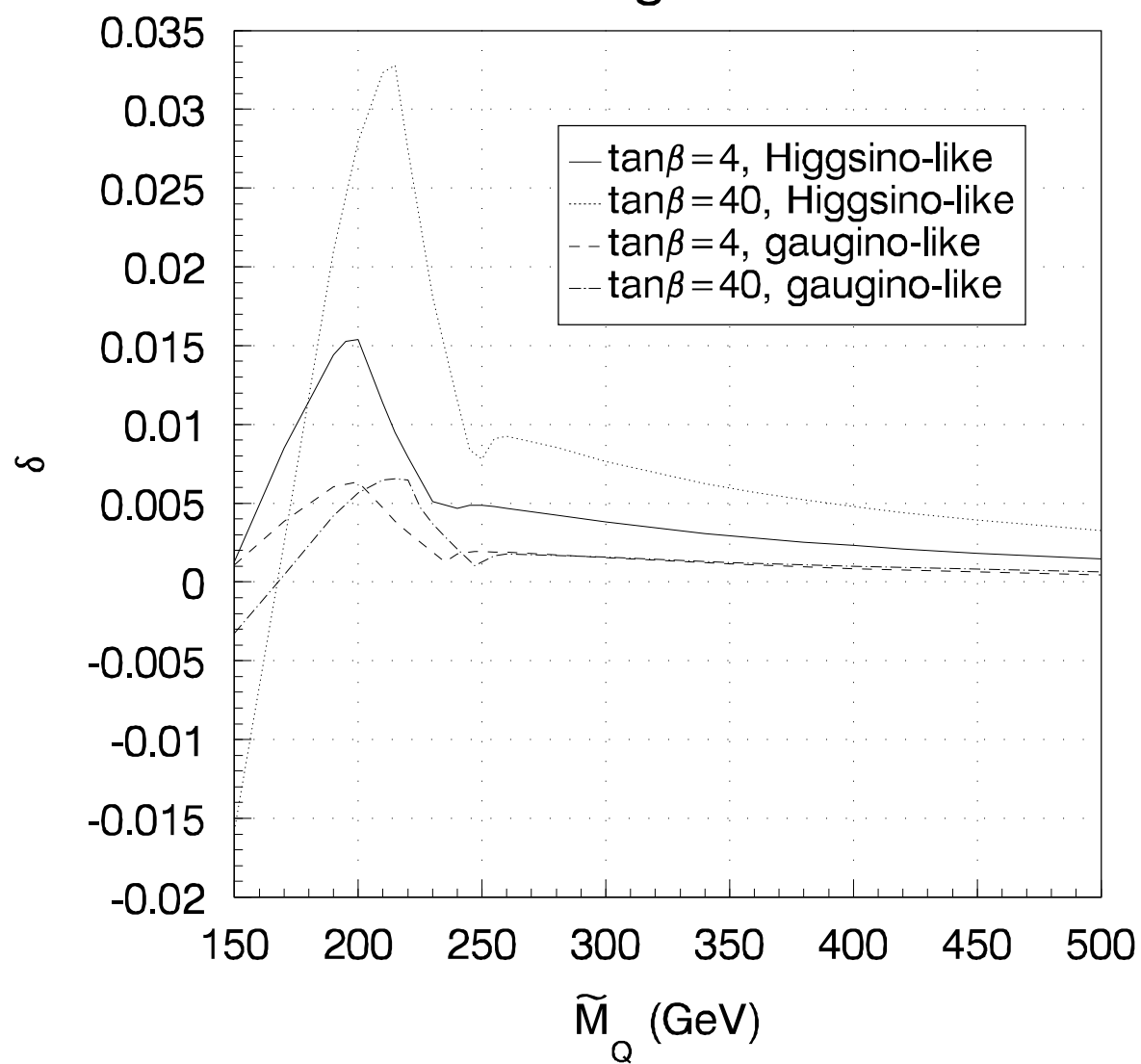


Fig.5

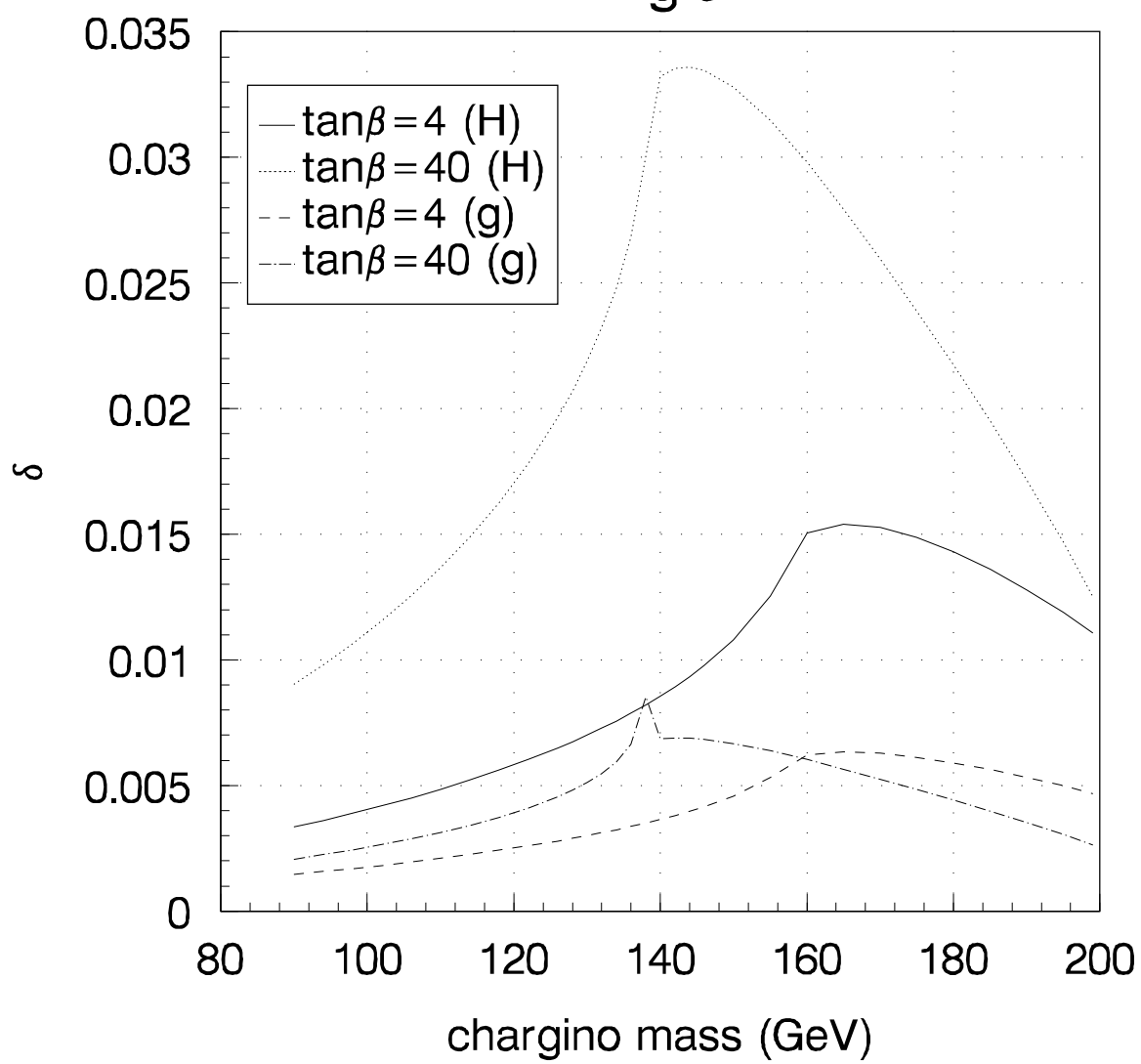


Fig.6

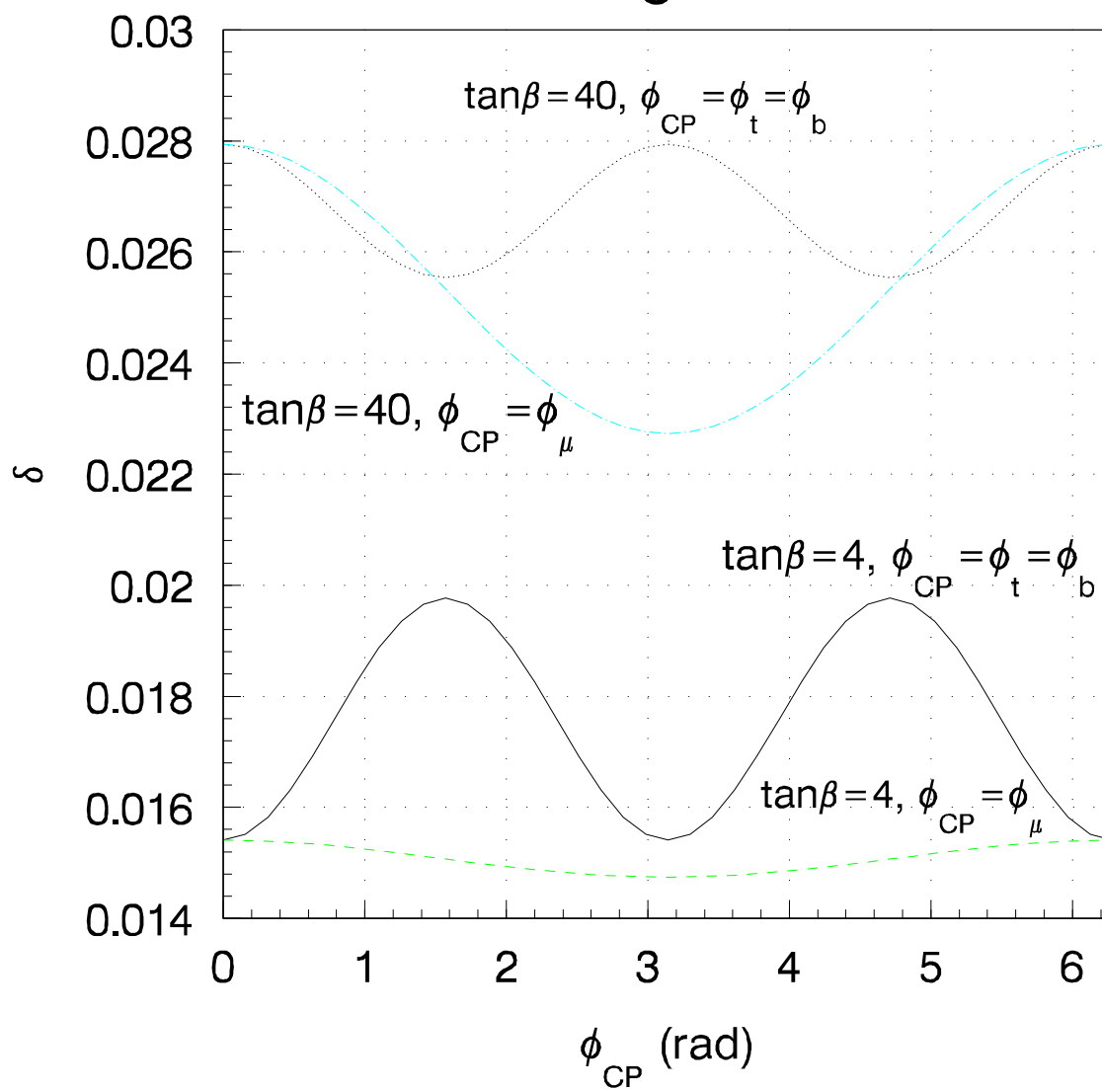


Fig.7(a)

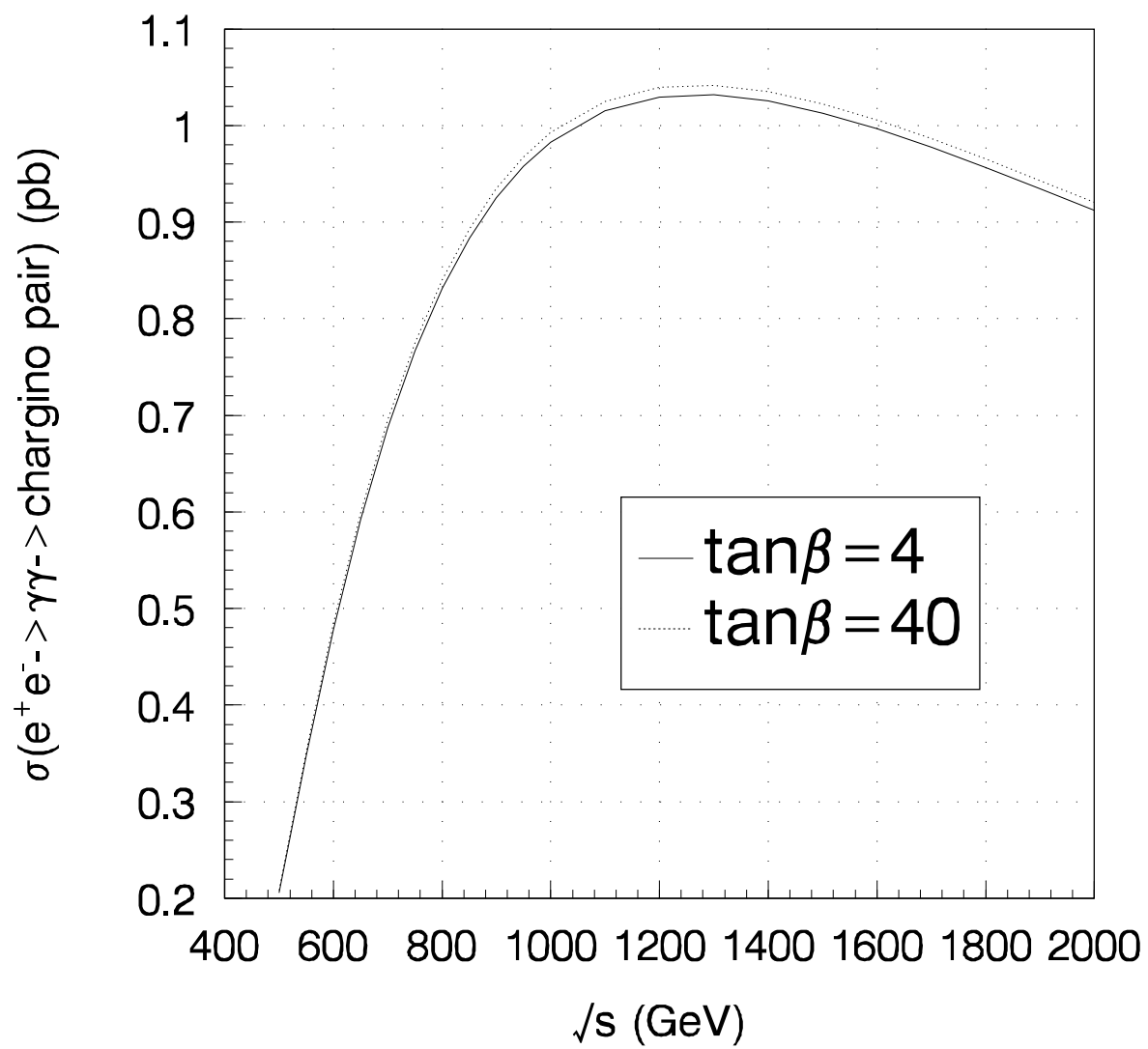


Fig.7(b)

